ORGANOMETALLICS

Article

Cite This: *Organometallics* 2017, 36, 4990−5002

Allosteric Effects in Ethylene Polymerization Catalysis. Enhancement of Performance of Phosphine-Phosphinate and Phosphine-Phosphonate Palladium Alkyl Catalysts by Remote Binding of $B(C_6F_5)_3$

Alison M. Johnson, Nathan D. Contrella, Jessica R. Sampson, Mingfang Zheng, and Richard F. Jordan*

Department of Chemistry, University of Chicago, 5735 S. Ellis Avenue, Chicago, Illinois 60637, United States

Supporting Information

ABSTRACT: Remote binding of $B(C_6F_5)_3$ to (PPO)PdMeL (L = pyridine or lutidine) or $\{(PPO)PdMe\}_2$ ethylene polymerization catalysts that contain phosphine-arenephosphinate or phosphine-arenephosphonate ligands (PPO^- = [1-PAr_2-2-$PR'O_2$-Ph]$^-$: Ar = R′ = Ph (**1a**); Ar = Ph, R′ = OEt (**1b**); Ar = Ph, R′ = O^{i}Pr (**1c**); Ar = 2-OMe-Ph, R′ = O^{i}Pr (**1d**)) significantly increases the catalyst activity and the molecular weight of the polyethylene (PE) product. In the most favorable case, *in situ* conversion of (**1d**)PdMe(py) to the base-free adduct {**1d**·$B(C_6F_5)_3$}PdMe increases the ethylene polymerization activity from 9.8 to 5700 kg mol^{-1} h^{-1} and the M_n of the PE product from 9030 to 99 200 Da (80 °C, 410 psi). X-ray structural data, trends in ligand lability, and comparative studies of BF_3 activation suggest that these allosteric effects are primarily electronic in origin. The $B(C_6F_5)_3$ binding enhances the chain growth rate (R_{growth}) by increasing the degree of positive charge on the Pd center. This effect does not result in the large increase in the chain transfer rate ($R_{transfer}$) and concomitant reduction in PE molecular weight seen in previous studies of analogous (PO)PdRL catalysts that contain phosphine-arene*sulfonate* ligands, because of the operation of a dissociative chain transfer process, which is inhibited by the increased charge at Pd.

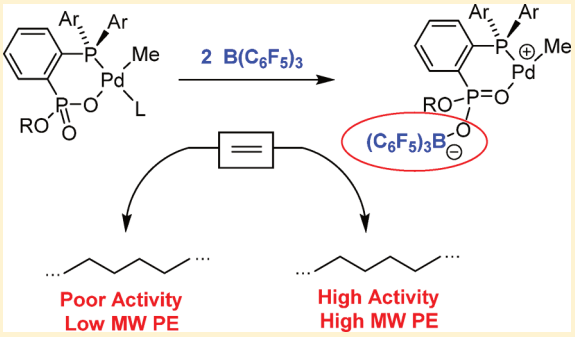

INTRODUCTION

Pd(II) alkyl complexes that contain ancillary *ortho*-phosphine-arenesulfonate (PO^-) ligands (**A**, Chart 1) polymerize ethylene to linear polyethylene (PE) and copolymerize ethylene with a wide variety of polar vinyl monomers.[1−3] While the broad functional group tolerance of these catalysts is unique, their activities and the molecular weights (MWs) of the polymers they produce are generally much lower than those of other single-site catalysts,[4] which has motivated extensive modifications of the PO^- ligand structure to enhance catalyst performance. Noteworthy examples of superior (PO)PdMeL catalysts include (*o*-P^{t}BuPh-benzenesulfonate)PdMe(lut) (lut = 2,6-lutidine), which exhibits high ethylene polymerization activity for this class of catalysts (4714 kg mol^{-1} h^{-1}, 85 °C),[2o] (*o*-P(menthyl)$_2$-benzenesulfonate)PdMe(lut), which produces PE with high MW (M_n = 169 000 Da, 80 °C),[2j] and (*o*-P(2′,6′-(OMe)$_2$-2-biphenyl)$_2$-benzenesulfonate)PdMe-(lut), which displays a good balance of activity and MW (1040 kg mol^{-1} h^{-1}; M_n = 227 000 Da, 90 °C).[2p] Analogues of (PO)PdMeL catalysts in which the sulfonate group has been replaced by other weak donors have also been explored,[5−9] including systems that contain phosphine-trifluoroborate,[5] phosphine-sulfonamide,[6] phosphine-phosphine oxide,[7] phosphine-dialkyl phosphonate,[8] and phosphine-phosphonamide ligands.[9] The phosphine-phosphonamide complex **B** with R^1 = *o*-OMe-Ph, R^2 = ^{i}Pr, and R^3 = Ph is one of most active (PO)Pd-type catalysts for ethylene polymerization (6000 kg mol^{-1} h^{-1}, 80 °C) reported to date and produces PE with high MW (130 000 Da).[10]

An alternative approach to improving catalytic performance is allosteric regulation, i.e., binding of a small "effector" molecule at a location remote from the active site to induce structural/conformational changes that regulate activity.[11,12] This concept has been implemented in synthetic catalysts for asymmetric hydrogenation,[12a] asymmetric hydroformylation,[12b] Diels−Alder reactions,[12c] and other reactions,[12d−k] as well as olefin polymerization catalysis.[12l,m,13] In particular, Bazan reported that coordination of $B(C_6F_5)_3$ to (*o*-PPh_2-benzoate)-Ni(η^3-CH_2CMeCH_2) to form zwitterionic complex **C** results in a significant increase in the ethylene oligomerization activity of this system.[13a,b] Similar binding of $B(C_6F_5)_3$ to inactive (α-iminocarboxamide)Ni(η^3-CH_2Ph) complexes to form adducts **D** activates these species for ethylene polymerization.[13c] More recently, binding of $B(C_6F_5)_3$ to the sulfonate oxygen of (PO)PdRL complexes to form zwitterionic {PO·B$^-$(C_6F_5)$_3$}-Pd$^+$RL species (**E**)[14] was found to increase the rate of chain growth (R_{growth}) in ethylene polymerization, leading to higher

Received: November 8, 2017
Published: November 28, 2017

DOI: 10.1021/acs.organomet.7b00815
Organometallics 2017, 36, 4990−5002

Chart 1. (PO)PdRL-Type Complexes

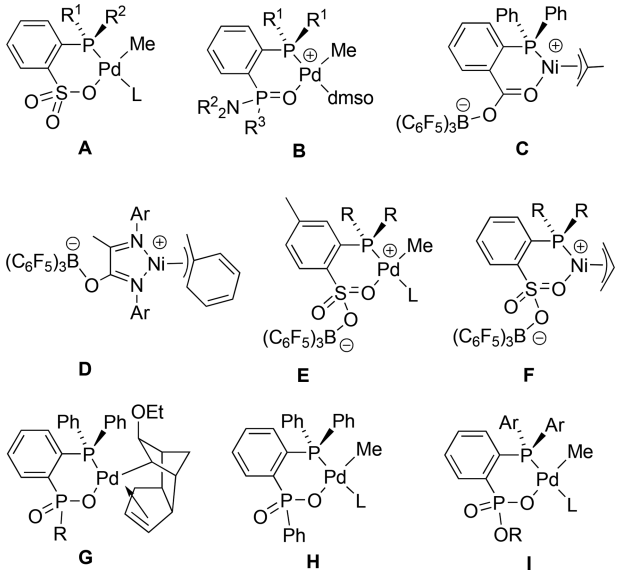

activities. However, the borane coordination in **E** also results in larger increases in the rate of chain transfer ($R_{transfer}$), so that the $R_{growth}/R_{transfer}$ ratio and hence the MW of the PE that is produced is substantially reduced. For example, coordination of $B(C_6F_5)_3$ to a sulfonate oxygen of (o-P(2-Et-Ph)$_2$-benzenesulfonate)PdMe(py) leads to a 4-fold increase in R_{growth} but a 42-fold increase in $R_{transfer}$ and thus a ca. 10-fold reduction in M_n. In contrast, coordination of $B(C_6F_5)_3$ to (PO)Ni(allyl) complexes to form {PO·B$^-$(C_6F_5)$_3$}Ni$^+$(allyl) complex (**F**) has very little effect on the ethylene polymerization performance.[12m]

Reiger reported neutral compounds **G** that contain phosphine-phosphinate (R = Ph) and phosphine-phosphonate (R = OH) ligands (PPO$^-$).[15] These complexes are unreactive with ethylene.[16] The lack of reactivity may result from a high barrier to opening of the alkyl-olefin chelate by ethylene coordination or may be an inherent characteristic of the PPO$^-$ ligand.

In this paper, we report simple (PPO)PdMeL complexes that contain phosphine-phosphinate (**H**) and phosphine-monoalkyl phosphonate (**I**, R = Et, ^{i}Pr) ligands. These complexes exhibit low activity in ethylene polymerization. We show that allosteric binding of $B(C_6F_5)_3$ to the P═*O* group of **H** and **I** to generate zwitterionic (PPO·B$^-$(C_6F_5)$_3$}Pd$^+$MeL adducts leads to increases in both R_{growth} and the $R_{growth}/R_{transfer}$ ratio, resulting in substantial increases in *both* catalyst activity and the MW of the PE product, and, in one case, overall ethylene polymerization performance that rivals that of the best (PO)PdRL-type systems.

RESULTS AND DISCUSSION

Synthesis of (κ^2-1-*P*Ph$_2$-2-P(═O)(*O*)Ph-Ph)PdMe(lut). The sequential reaction of the phosphine-phosphinate proligand 1-PPh$_2$-2-PO(OH)Ph-Ph (H[**1a**])[15] with (TMEDA)PdMe$_2$ and 2,6-lutidine affords (**1a**)PdMe(lut) (**2a-lut**, Scheme 1).

The molecular structure of **2a-lut** is shown in Figure 1. The O1−P2 bond (1.518(4) Å) is longer than the O2−P2 bond (1.462(4) Å), consistent with the resonance structure in Scheme 1. These bond distances are comparable to those in P(O)(OH)Ph$_2$ (P−OH 1.526(6) Å, P═O 1.486(6) Å)[17] and P(O)(O^{t}Bu)Ph$_2$ (P−O^{t}Bu 1.569(3) Å, P═O 1.476(3) Å).[18]

Scheme 1. Synthesis of 2a-lut

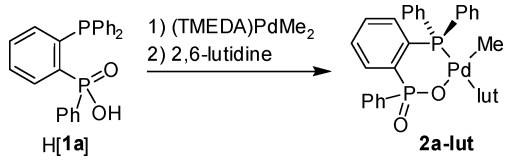

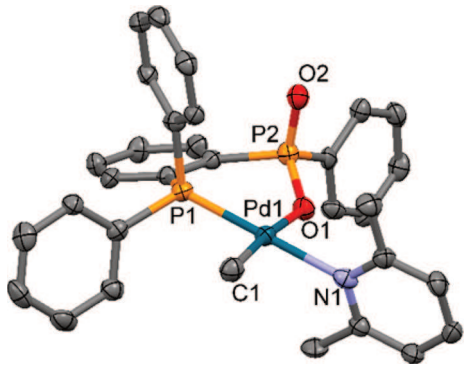

Figure 1. Molecular structure of **2a-lut**·CH_2Cl_2. The CH_2Cl_2 molecule and hydrogen atoms are omitted. Bond lengths (Å) and angles (deg): C1−Pd1 2.006(6), N1−Pd1 2.119(5), O1−Pd1 2.097(4), P1−Pd1 2.1977(17), O1−P2 1.518(4), O2−P2 1.462(4), C1−Pd1−N1 89.8(2), N1−Pd1−O1 86.09(16), O1−Pd1−P1 94.45(11), P1−Pd1−C1 89.68(17).

Spontaneous Loss of 2,6-Lutidine from 2a-lut. The $^{31}P\{^1H\}$ NMR spectrum of **2a-lut** in CD_2Cl_2 solution contains two sets of resonances, indicating that two species are present. One of these species exhibits two sharp doublets at δ 31.4 and 17.5 ($^3J_{PP}$ = 15 Hz) as expected for **2a-lut**, and the other gives rise to two broad signals in the same range (Figure 2a).

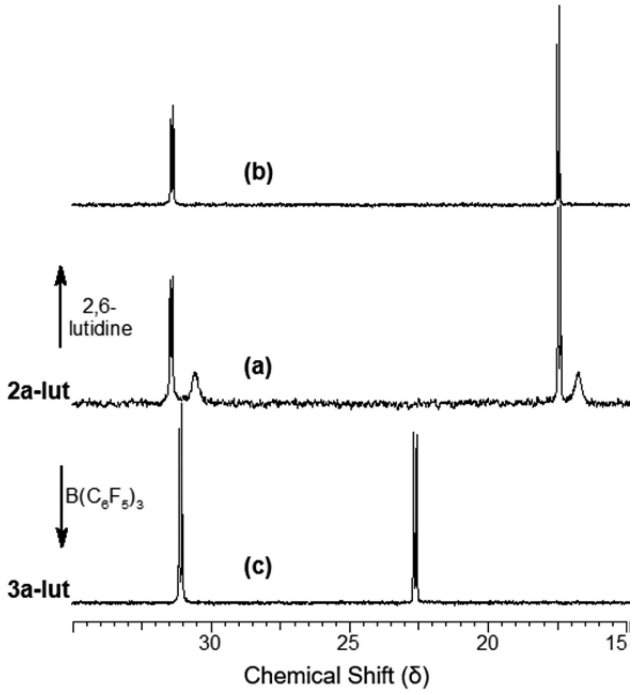

Figure 2. $^{31}P\{^1H\}$ NMR spectra of **2a-lut** (a) in CD_2Cl_2 at room temperature, (b) upon addition of excess 2,6-lutidine, and (c) upon addition of 1 equiv of $B(C_6F_5)_3$.

DOI: 10.1021/acs.organomet.7b00815
Organometallics 2017, 36, 4990−5002

Resonances for free 2,6-lutidine are observed in the ^{1}H NMR spectrum, and CD_2Cl_2 solutions of **2a-lut** slowly deposit solid. Addition of excess 2,6-lutidine dissolves the solid and converts the broad signals to the sharp doublets (Figure 2b). These observations indicate that **2a-lut** undergoes partial dissociation of 2,6-lutidine to form a poorly soluble base-free species (Scheme 2), which is likely dimeric based on the structures of base-free (PO)PdR species.[2g,14,19]

Scheme 2. Synthesis of 3a-lut

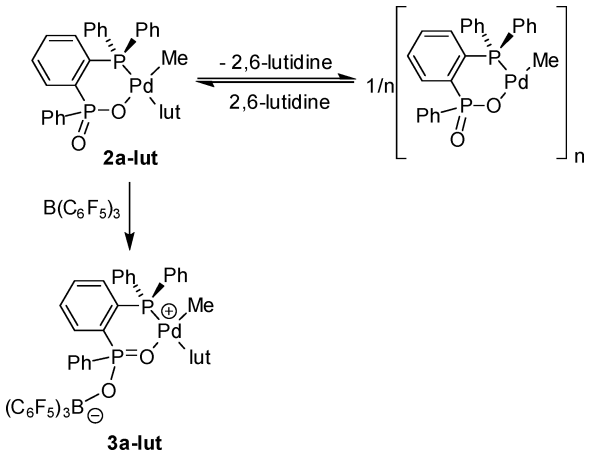

Binding of $B(C_6F_5)_3$ to 2a-lut. The addition of $B(C_6F_5)_3$ to a CD_2Cl_2 solution of **2a-lut** results in the disappearance of the NMR resonances for the $\{(PO)PdR\}_n$ species and free lutidine, dissolution of the solid, and quantitative formation of the adduct $\{$**1a**·$B(C_6F_5)_3\}$PdMe(lut) (**3a-lut**). The $^1P\{^1H\}$ NMR spectrum of **3a-lut** displays two sharp doublets at δ 31.1 and 22.7 ($^3J_{PP}$ = 15 Hz, Figure 2c). The low-field shift of the phosphinate ^{31}P resonance (δ 22.7) and the preservation of resonances for Pd-coordinated 2,6-lutidine in the ^{1}H NMR spectrum indicate that $B(C_6F_5)_3$ binds to a phosphinate oxygen atom, as shown in Scheme 2. Complex **3a-lut** was synthesized on a preparatory scale by the reaction of **2a-lut** and $B(C_6F_5)_3$ in CH_2Cl_2, and its structure was confirmed by X-ray diffraction (Figure 3).

The O2–P2 bond of **3a-lut** is ca. 0.05 Å longer than the O1–P2 bond, indicating that the bonding is best represented by the resonance structure in Scheme 2. The O1–Pd1 distance in **3a-lut** is ca. 0.04 Å longer than that in **2a-lut**, consistent with the expected decrease in the donor ability of the phosphinate ligand upon $B(C_6F_5)_3$ binding. However, the Pd–Me distances in the two complexes are not significantly different. The $B(C_6F_5)_3$ coordination induces inversion of the conformation of the (PPO)Pd chelate ring, which moves the phosphinate phenyl ring from an equatorial position in **2a-lut** to an axial position in **3a-lut**. One C_6F_5 ring (C39–C44), the phosphinate phenyl ring (C27–C32), and a phosphine phenyl ring (C15–C20) are organized in a triple-decker π-stacked arrangement.[20,21]

Synthesis of (κ^2-1-*P*Ar_2-2-P(=O)(*O*)(OR)-Ph)PdMeL Complexes. The phosphine-phosphonate diesters 1-PAr_2-2-$PO(OR)_2$-Ph (**4b**: Ar = Ph, R = Et; **4c**: Ar = Ph, R = ^{i}Pr; **4d**: Ar = 2-OMe-Ph = An, R = ^{i}Pr); see the Supporting Information for synthesis)[15,22,23] were mono-dealkylated by reaction with LiBr in refluxing CH_3CN, affording Li[**1b–d**] (Scheme 3),[24] and then acidified with HCl to generate the phosphine-phosphonate monoester proligands H[**1b–d**].

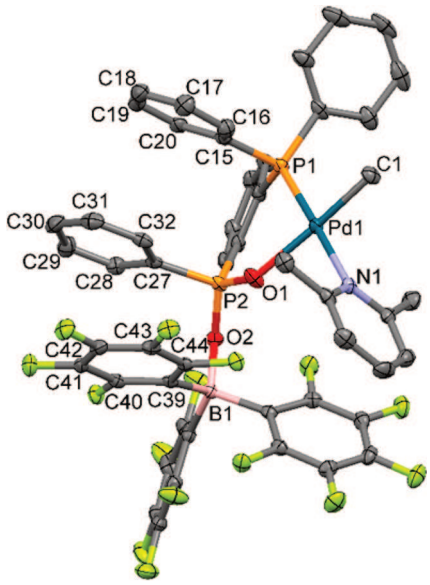

Figure 3. Molecular structure of **3a-lut**. Hydrogen atoms are omitted. Bond lengths (Å) and angles (deg): C1–Pd1 2.021(2), N1–Pd1 2.1272(17), O1–Pd1 2.1416(14), P1–Pd1 2.2110(6), O1–P2 1.4876(15), O2–P2 1.5361(15), C1–Pd1–N1 90.59(8), N1–Pd1–O1 88.35(6), O1–Pd1–P2 89.88(4), P2–Pd1–C1 91.27(6).

Scheme 3. Synthesis of Phosphine-Phosphonate Ligands

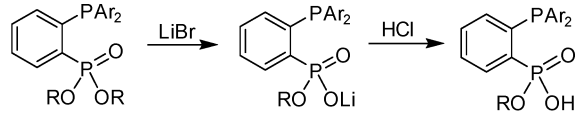

The sequential reaction of H[**1b**], H[**1c**], or H[**1d**] with (TMEDA)$PdMe_2$, followed by 2,6-lutidine or pyridine, affords the corresponding (PPO)PdMeL complexes (L = 2,6-lutidine: **2b-lut**, **2c-lut**; L = pyridine: **2b-py**, **2c-py**, **2d-py**) as shown in Scheme 4. Chelation of the PPO^- ligand is indicated by the

Scheme 4. Synthesis of Phosphine-Phosphonate Pd Complexes

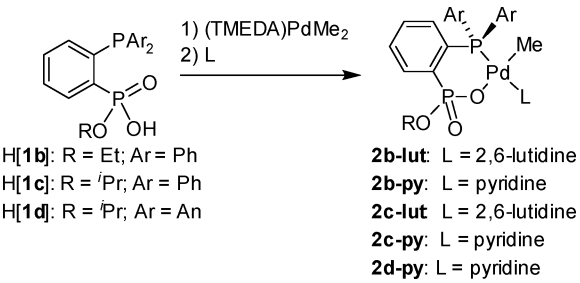

presence of P–P coupling in the $^{31}P\{^1H\}$ NMR spectra of **2b-lut/py**, **2c-lut/py**, and **2d-py** ($^3J_{PP}$ = 14–17 Hz), which is not observed in the spectra of the free ligands. Selective ^{31}P-decoupled ^{1}H NMR spectra of **2c-py** were used to assign the phosphine (δ 8.6) and phosphonate (δ 32.4) ^{31}P resonances. The solid-state molecular structures of **2b-lut** and **2c-lut** are shown in Figures 4 and 5 and are similar to that of **2a-lut**, with the P-*OR* groups occupying axial positions on the chelate ring.

DOI: 10.1021/acs.organomet.7b00815
Organometallics 2017, 36, 4990–5002

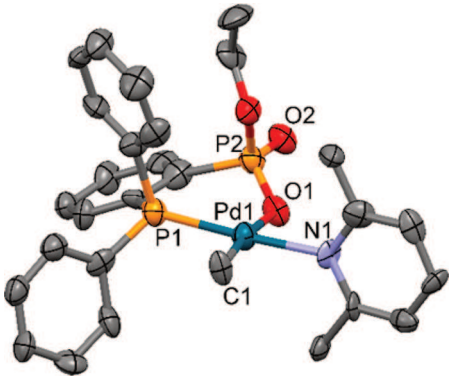

Figure 4. Molecular structure of **2b-lut**·CH_2Cl_2. The CH_2Cl_2 molecule and hydrogen atoms are not shown. Bond lengths (Å) and angles (deg): C1−Pd1 2.016(10), N1−Pd1 2.096(9), O1−Pd1 2.103(7), P1−Pd1 2.197(3), O2−P2 1.462(8), O1−P2 1.497(8), C1−Pd1−N1 84.5(4), N1−Pd1−O1 90.6(3), O1−Pd1−P1 94.9(2), P1−Pd1−C1 90.3(3).

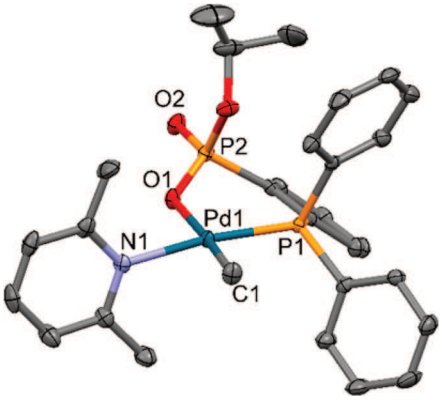

Figure 5. Molecular structure of **2c-lut**·CH_2Cl_2·$0.5H_2O$. The CH_2Cl_2 and H_2O molecules and hydrogen atoms are not shown. Bond lengths (Å) and angles (deg): C1−Pd1 2.030(3), N1−Pd1 2.124(3), O1−Pd1 2.138(2), P1−Pd1 2.2104(9), O2−P2 1.487(2), O1−P2 1.507(2), C1−Pd1−N1 87.98(12), N1−Pd1−O1 86.96(9), O1−Pd1−P1 96.73(6), P1−Pd1−C1 88.76(10).

As observed for **2a-lut**, **2b-lut** and **2c-lut** undergo partial dissociation of 2,6-lutidine in CD_2Cl_2 solution, which is indicated by the presence of minor signals for free lutidine and minor broad signals ascribed to base-free $\{(PPO)PdMe\}_n$ species in the ^1H NMR spectra.[25]

$B(C_6F_5)_3$ Binding to 2b-lut. The reaction of **2b-lut** with $B(C_6F_5)_3$ affords the *O*-bound borane adduct $\{$**1b**·$B(C_6F_5)_3\}$-PdMe(lut) (**3b-lut**, Scheme 5), the structure of which is shown in Figure 6. Consistent with the results for **2a-lut** and **3a-lut**, the Pd1−O1 distance in **3b-lut** is ca. 0.04 Å longer than that in **2b-lut** due to the decreased donor ability of the $B(C_6F_5)_3$-coordinated phosphonate group. However, in this case, the borane does not induce a change in the conformation of the (PPO)Pd chelate ring, and the ethoxy group occupies an axial site.

Synthesis of Base-Free $B(C_6F_5)_3$-Coordinated $\{$[PPO·$B(C_6F_5)_3$]PdMe$\}_2$ Complexes. The reaction of **2b-py** with 2 equiv of $B(C_6F_5)_3$ yields the base-free, borane-coordinated species $\{$[**1b**·$B(C_6F_5)_3$]PdMe$\}_2$ as a mixture of two diastereomers, **5b** and **5b′**, which differ in the relative configurations of the phosphonate phosphorus atoms (Scheme 5). The $^{19}F\{^1H\}$ and ^1H NMR spectra of **5b**/**5b′** each contain two sets

Scheme 5. Synthesis of $B(C_6F_5)_3$ Adducts

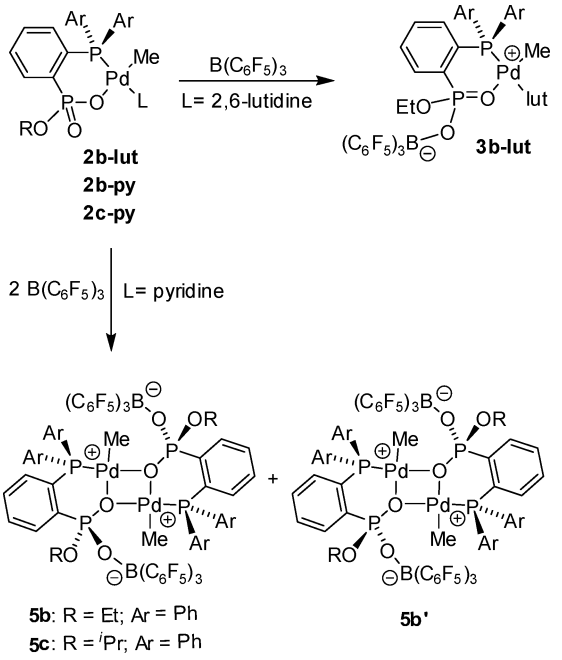

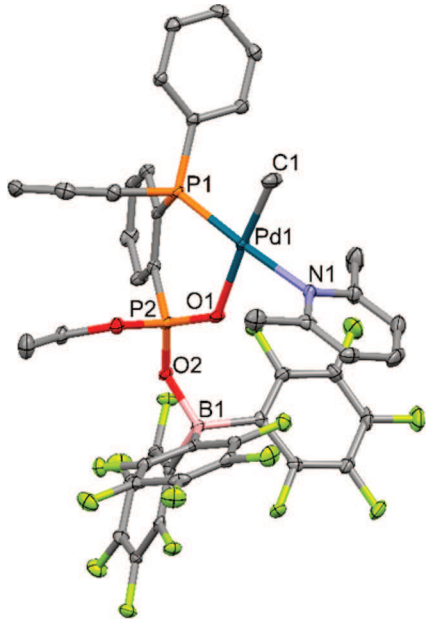

Figure 6. Molecular structure of **3b-lut**·CH_2Cl_2. The CH_2Cl_2 molecule and hydrogen atoms are omitted. Bond lengths (Å) and angles (deg): C1−Pd1 2.034(3), N1−Pd1 2.115(2), O1−Pd1 2.1400(19), P1−Pd1 2.2166(8), O1−P2 1.483(2), O2−P2 1.573(2), C1−Pd1−N1 89.49(11), N1−Pd1−O1 85.25(8), O1−Pd1−P1 94.92(6), P1−Pd1−C1 90.51(9).

of resonances in an 80/20 intensity ratio for the two isomers. Isomer **5b′**, which has *S,S* (*ent-R,R*) configurations at the phosphonate centers, was isolated by recrystallization from $CHCl_2CHCl_2/CH_2Cl_2$/hexanes as a racemic conglomerate and identified by X-ray diffraction (Figure 7).[26] The two [**1b**·$B(C_6F_5)_3$]PdMe units are linked through a four-membered Pd1−O1−Pd1A−O1A ring. A similar structure was observed previously for $\{2\text{-}P(3,5\text{-}^tBu_2\text{-}Ph)_2\text{-}p\text{-}$toluenesulfonate$)Pd\text{-}Me\}_2$.[14] The conformation of the (PPO)Pd chelate ring in **5b′** is similar to that in **3b**, with the ethoxy group occupying an

DOI: 10.1021/acs.organomet.7b00815
Organometallics 2017, 36, 4990−5002

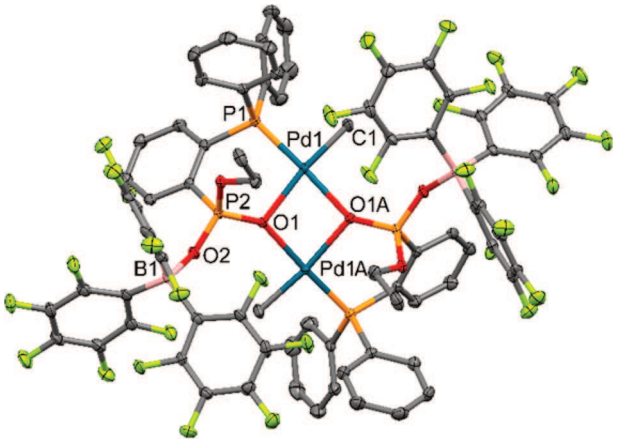

Figure 7. Molecular structure of **5b′**·CH_2Cl_2·$CHCl_2CHCl_2$. The CH_2Cl_2 and $CHCl_2CHCl_2$ molecules and hydrogen atoms are omitted. Bond lengths (Å) and angles (deg): C1−Pd1 2.005(3), O1−Pd1 2.1539(19), P1−Pd1 2.1802(8), O1A−Pd1 2.2049(19), P2−O1 1.512(2), P2−O2 1.511(2), O1−Pd1−O1A 79.16(8), O1A−Pd1−C1 93.12(11), C1−Pd1−P1 89.14(10), O1−Pd1−P1 98.59(5), Pd1−O1−Pd1A 94.14(7).

axial position. Addition of 1 equiv of 2,6-lutidine or a coordinating solvent converts **5b**/**5b′** back to the corresponding {**1b**·$B(C_6F_5)_3$}PdMeL species.

Similarly, the base-free dimer {[**1c**·$B(C_6F_5)_3$]PdMe}$_2$ (**5c**) was synthesized by the reaction of **2c-py** with 2 equiv of $B(C_6F_5)_3$ in CH_2Cl_2 (Scheme 5). In this case, only one isomer is observed in the NMR spectra. An X-ray diffraction analysis shows that **5c** has *S*,*R* configurations at the phosphonate centers (Figure 8). The borane coordination induces a significant change in the conformation of the (PPO)Pd chelate from the boat observed for **2c-lut** to an envelope in which the −O^{i}Pr and −O$B(C_6F_5)_3$ groups lie above and below Pd1−O1−P2−C9−C8 plane (Figure 9). A π-stacking interaction between a C_6F_5 ring (C23−C28) and the backbone arene ring of the

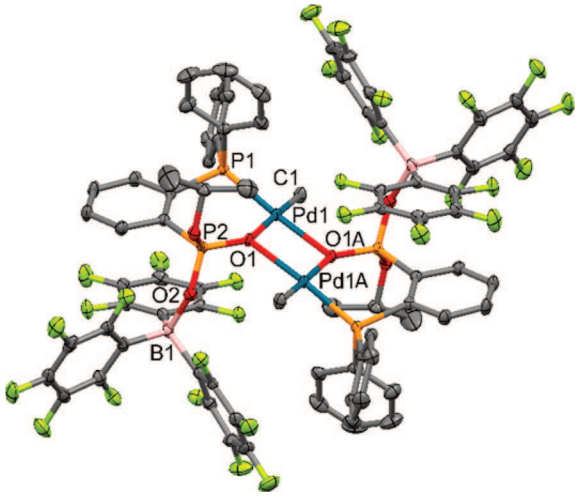

Figure 8. Molecular structure of **5c**. Hydrogen atoms are omitted. Bond lengths (Å) and angles (deg): C1−Pd1 2.021(3), O1−Pd1 2.2057(19), P1−Pd1 2.1876(8), O1A−Pd1 2.2284(19), P2−O1 1.513(2), P2−O2 1.510(2), O1−Pd1−O1A 82.90(8), O1A−Pd1−C1 96.38(10), C1−Pd1−P1 89.64(9), O1−Pd1−P1 91.55(5), Pd1−O1−Pd1A 97.10(8).

PPO$^-$ ligand (C8−C12) is associated with this conformational change.[27]

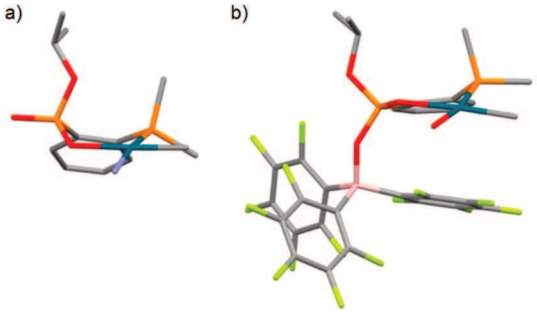

Figure 9. Molecular structures highlighting the change in the (κ^2-*P*,*O*)Pd chelate ring conformation from (a) boat in **2c-lut** to (b) envelope in **5c**. Hydrogens, P*Ph*$_2$ groups, 2,6-lutidine carbons in **2c-lut**, and half of the dimer in **5c** have been removed for clarity.

Ethylene Polymerization. Complexes **2a-lut**, **2b-lut**/**py**, and **2c-lut**/**py** exhibit very low activity for ethylene polymerization (0.7−3.5 kg mol^{-1} h^{-1}) and produce PE with M_n < 5340 Da (Table 1, entries 1, 4, 6, 11, 12). Complex **2d-py**, which

Table 1. Ethylene Polymerization by (PPO)PdMeL and {PPO·$B(C_6F_5)_3$}PdMeL Catalysts[a]

entry	catalyst	$B(C_6F_5)_3$ (equiv)	act.[b]	M_n[c]	PDI[c]	T_m (°C)[d]
1	**2a-lut**	0	0.7	1340	1.35	120.0
2[e]	**3a-lut**	0	35	7770	1.71	128.5
3[e]	**3a-lut**	1	175	6670	1.98	128.6
4[e]	**2b-lut**	0	3.5	3350	1.84	129.2
5[e]	**2b-lut**[f]	0	2.0	2620	1.81	128.1
6[e]	**2b-py**	0	2.4	1480	1.90	124.3
7[e]	**2b-py**[g]	0	248	4140	2.03	132.6
8[e]	**3b-lut**	0	50	7260	1.98	132.2
9[e]	**3b-lut**	1	335	7910	1.91	132.8
10[e]	**5b**/**5b′**[h,i]	0	308	6370	2.23	132.1
11[e]	**2c-lut**	0	2.1	5340	1.38	131.0
12[e]	**2c-py**	0	1.8	1360	1.65	123.4
13[e]	**5c**[h,i]	0	529	10300	1.86	133.2
14[e]	**2d-py**	0	9.8	9030	1.34	131.2
15[e]	**2d-py**[h]	2	3390	91200	2.11	135.9
16	**2d-py**[h]	4	5330	96400	2.21	137.0
17	**2d-py**[h]	8	5700	99200	2.14	136.1

[a]Conditions: 50 mL of toluene, 10 μmol of Pd, 80 °C, 410 psi ethylene, 2 h, unless otherwise noted. [b]Activity in kg mol^{-1} h^{-1}. [c]Determined by GPC. [d]Determined by DSC. [e]Average of at least two reactions. [f]28 μmol of Pd, 450 psi, 21 h. [g]2 equiv of BF_3·Et_2O added. [h]0.88 μmol of Pd. [i]450 psi.

contains a PAn_2 unit in the PPO$^-$ ligand, is somewhat more active (9.8 kg mol^{-1} h^{-1}) and produces PE with M_n = 9030 Da (entry 14), but the performance of all of these catalysts is quite poor relative to that of analogous (PO)PdRL catalysts.[19,28] Polymerizations run for a longer time with **2b-lut** (entry 5) retained approximately the same activity, indicating that these catalysts are reasonably stable under the polymerization conditions. These findings indicate that the catalytic ability of (PPO)PdR complexes is innately poor, consistent with previous results for catalysts of type **G**.[15,16]

DOI: 10.1021/acs.organomet.7b00815
Organometallics 2017, 36, 4990−5002

Table 2. Examples of High-Performance PO-Type Catalysts for Ethylene Polymerization

entry	complex	act.[a]	M_n
1	**2d-py** + 8 $B(C_6F_5)_3$	5700	99200
2[b]	(*o*-P(2-Et-Ph)$_2$-*p*-toluenesulfonate)PdMe(py) + 4 $B(C_6F_5)_3$	5650	2520
3[c]	(*o*-(P^{t}BuPh)-benzenesulfonate)PdMe(lut)	4714	14600
4[d]	(*o*-P(menthyl)$_2$-benzenesulfonate)PdMe(lut)	205	169000
5[e]	(*o*-P(2′,6′-(OMe)$_2$-2-biphenyl)$_2$-benzenesulfonate)PdMe(lut)	1040	227000
6[f]	(*o*-P(2′,6′-(OMe)$_2$-2-biphenyl)$_2$-benzenesulfonate)PdMe	5330	29000
7[g]	(*o*-PAn$_2$-naphthalenesulfonate)PdMe(dmso)	3900	16000
8[h]	[{*o*-(P^{i}Pr$_2$)C$_6$H$_4$(P(O)^{t}Bu$_2$)}Pd(κ^2-*o*-acetanilido)]$^+$[B(3,5-(CF$_3$)$_2$-Ph)$_4$]$^-$	2800	29000
9[i]	[{*o*-(PAn$_2$)C$_6$H$_4$(P(O)(N(^{i}Pr)$_2$)Ph)}PdMe(dmso)]$^+$[B(3,5-(CF$_3$)$_2$-Ph)$_4$]$^-$ (**B**)	3500	190000

[a]Activity in kg mol^{-1} h^{-1}. [b]Conditions: 50 mL of toluene, 1.0 μmol of Pd, 435 psi ethylene, 80 °C, 1 h, ref 14. [c]Conditions: 200 mL of toluene, 6.5 μmol of Pd, 300 psi ethylene, 85 °C, 1 h, ref 2o. [d]Conditions: 100 mL of toluene, 10 μmol of Pd, 435 psi ethylene, 80 °C, 1 h, ref 2j. [e]Conditions: 200 mL of toluene, 10 μmol of Pd, 300 psi ethylene, 80 °C, 1 h, ref 2p. [f]Conditions: 100 mL of toluene, 4 μmol of Pd, 5 bar ethylene, 80 °C, 0.5 h, ref 2n. [g]Conditions: 48 mL of toluene, 2 mL of CH_2Cl_2, 0.4 μmol of Pd, 9 atm ethylene, 90 °C, 1 h, ref 2q. [h]15 mL of toluene, 0.75 μmol of Pd, 435 psi ethylene, 100 °C, 1 h, ref 8. [i]Conditions: 48 mL of toluene, 2 mL of CH_2Cl_2, 1 μmol of Pd, 132 psi ethylene, 80 °C, 1 h, ref 9.

However, coordination of $B(C_6F_5)_3$ to **2a-lut** and **2b-lut** significantly increases the catalytic activity and the MW of the PE product in both cases. The $B(C_6F_5)_3$ adducts **3a-lut** and **3b-lut** exhibit activities of 35−50 kg mol^{-1} h^{-1} and produce PE with M_n of ca. 7000 Da (entries 2 and 8). The activity of **3a-lut** and **3b-lut** can be further increased 5 to 7-fold by adding a second equivalent of $B(C_6F_5)_3$ to trap the 2,6-lutidine *in situ* or by using the isolated base-free, borane-coordinated dimer **5b**/**5b′** (entry 3 vs 2 and entries 9 and 10 vs 8). The M_n and α-olefin content (i.e., the polymer microstructure) of the PEs produced by **3a-lut** + $B(C_6F_5)_3$, **3b-lut** + $B(C_6F_5)_3$, and **5b**/**5b′** are similar to those observed in the absence of the additional borane, which implies that the second equivalent of $B(C_6F_5)_3$ traps the 2,6-lutidine but does not otherwise affect the active catalytic species. Similar, though less pronounced, effects on activity and MW are observed in ethylene polymerization by **2b-py** + 2 $BF_3{\cdot}Et_2O$, which is expected to form the BF_3-coordinated {**1b**·BF_3}PdMe(Et_2O) species and BF_3·py *in situ* (entry 7 vs 9 and 10).[29] Replacement of the ethoxy group of **5b**/**5b′** by the isopropoxy group in **5c** results in a ca. 65% increase in both the catalyst activity and the MW of the PE product (entry 13 vs 10). The catalyst **2d-py** + 2 $B(C_6F_5)_3$, which is expected to generate a base-free, borane-coordinated {**1d**·$B(C_6F_5)_3$}PdMe species analogous to **5b**/**5b′** and **5c** *in situ*, displays high activity (3390 kg mol^{-1} h^{-1}) and produces PE with M_n > 90 000 Da.

On the basis of previous studies of {PO·$B(C_6F_5)_3$}PdR borane adducts, it is probable that some dissociation of the borane occurs under the dilute concentration and high temperature conditions of ethylene polymerization reactions described above.[14] When excess $B(C_6F_5)_3$ (4 or 8 equiv) is added to **2d-py**-catalyzed ethylene polymerizations to counteract this effect, the activity and MW of the PE are increased further to 5700 kg mol^{-1} h^{-1} and 99 200 Da (entries 16 and 17).

The **2d-py** + 8 $B(C_6F_5)_3$ catalyst is one of the most active (PO)PdR-type catalysts reported to date that also produces high-MW PE (Table 2). The base-free borane adduct generated from (*o*-P(2-Et-Ph)$_2$-*p*-toluenesulfonate)PdMe(py) + 4 B-(C_6F_5)$_3$ exhibits similar activity but produces PE with low MW (entry 2).[14] Other **A**-type catalysts exhibit either high activity (entries 3, 6, 7, 8)[2n,o,q,7] or produce PE with high MW (entries 4 and 5).[2j,p] Under similar conditions to those reported here, the phosphine-phosphonamide complex **B** is the most comparable to **2d-py** + 8 $B(C_6F_5)_3$ in terms of both activity and MW (entry 9).[9]

The (PPO)PdR and {PPO·$B(C_6F_5)_3$}PdR catalysts reported here all produce linear PE with one olefin unit per saturated chain-end. The olefins comprise a mixture of terminal (17−46%) and internal (54−83%) olefins (see the Supporting Information). The internal olefins were characterized as 2- (60%), 3-(25%), and 4+-olefins (15%) by $^{13}C\{^1H\}$ NMR. To investigate whether these catalysts can isomerize α-olefins, 1-nonene was added to **2c-py** and **5c**-catalyzed ethylene polymerizations. No isomerization of the 1-nonene was detected by GC/MS analysis of the reaction mixtures. This result provides strong evidence that the internal olefins are formed during chain growth and not by post-polymerization isomerization of terminal olefins. These observations imply that (PPO)PdR and {PPO·$B(C_6F_5)_3$}PdR complexes can chain walk, but chain transfer is favored over insertion/growth for the resulting secondary alkyl species.

Influence of Ethylene Pressure. The ethylene polymerization behavior of **5b**/**5b′** was studied over a range of ethylene pressures from 50 to 850 psi. In this range, the activity of **5b**/**5b′** remains constant, with an average value of 306 kg mol^{-1} h^{-1} (Figure 10). This result is consistent with the catalyst resting state being the {PPO·$B(C_6F_5)_3$}PdR($CH_2{=}CH_2$) species.[4c] In contrast, the MW of the PE product increases

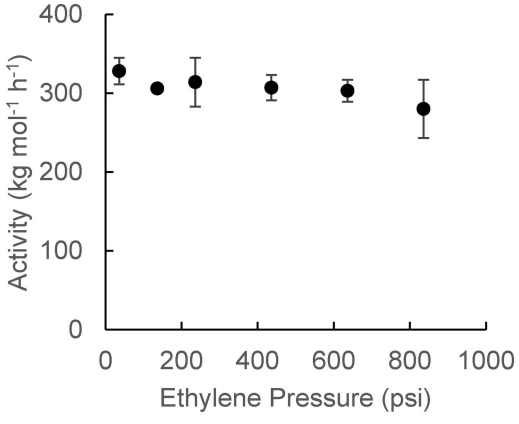

Figure 10. Effect of ethylene pressure on activity in ethylene polymerization by **5b**/**5b′**. Conditions: 50 mL of toluene, 0.88 μmol of Pd, 80 °C, 2 h. Each data point represents the average of two runs with error bars indicating high and low values.

DOI: 10.1021/acs.organomet.7b00815
Organometallics 2017, 36, 4990−5002

over this pressure range, with M_w increasing from 11 870 to 15 900 Da (Figure 11).

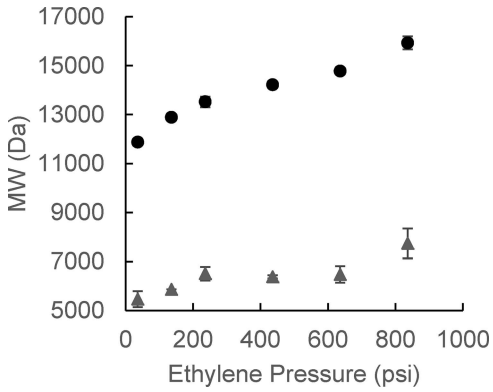

Figure 11. Effect of ethylene pressure on the MW of PE produced by **5b**/**5b′**. M_n data are shown as triangles and M_w data are shown as circles. Conditions: 50 mL of toluene, 0.88 μmol of Pd, 80 °C, 2 h. Each data point represents the average of two runs with error bars indicating high and low values. Molecular weights were determined by GPC.

The PE MW is determined by the $R_{growth}/R_{transfer}$ ratio (eq 1). The chain growth pathway and several possible chain transfer mechanisms for ethylene polymerization by **5b**/**5b′** are shown in Scheme 6. As noted above, the observation that activity is

Scheme 6. Chain Transfer Paths for (PO)Pd-Type Catalysts

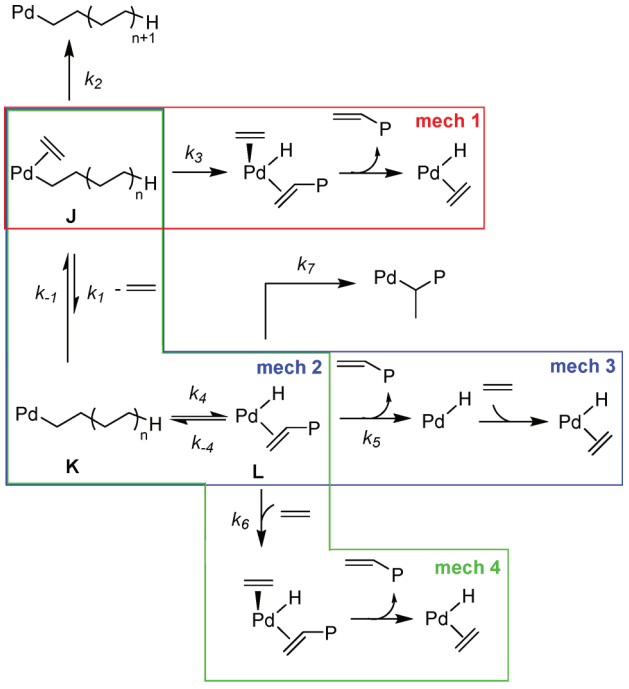

independent of ethylene pressure, i.e., R_{growth} is zero-order in ethylene concentration (eq 2), implies that the {PPO·$B(C_6F_5)_3$}PdR(CH_2=CH_2) species **J** is the catalyst resting state. A commonly assumed chain transfer process (mechanism 1) is β-H elimination from **J**, followed by dissociation of the unsaturated polymer chain. The rate of this chain transfer process ($R_{transfer,1}$) is zero-order in ethylene concentration (eq 3). Alternatively, chain transfer can occur through base-free species **K**, formed by dissociation of ethylene from **J**. From **K**, chain transfer can occur by β-H elimination to form Pd(olefin)(H) species **L**, followed by replacement of the unsaturated polymer chain by ethylene. Assuming pre-equilibrium conditions and k_4 as the rate-determining and irreversible step (mechanism 2), the rate of this chain transfer process ($R_{transfer,2}$) is inverse first-order in ethylene concentration (eq 4; see the Supporting Information). If β-H elimination by **J** is reversible and substitution of the unsaturated polymer chain of **L** by ethylene occurs by a dissociative mechanism (mechanism 3), the rate of chain transfer ($R_{transfer,3}$)

$$M_n = \frac{R_{growth}\cdot 28}{R_{transfer}} \quad (1)$$

$$R_{growth} = k_2[\mathbf{J}] \quad (2)$$

$$R_{transfer,1} = k_3[\mathbf{J}] \quad (3)$$

$$R_{transfer,2} = k_4[\mathbf{K}] = k_4K_1[\mathbf{J}][C_2H_4]^{-1} \quad (4)$$

where

$$K_1 = \frac{[\mathbf{K}][C_2H_4]}{[\mathbf{J}]}$$

$$R_{transfer,3} = k_5[\mathbf{L}] = k_5K_1K_4[\mathbf{J}][C_2H_4]^{-1} \quad (5)$$

where

$$K_4 = \frac{[\mathbf{L}]}{[\mathbf{K}]}$$

$$R_{transfer,4} = k_6K_1K_4[\mathbf{J}] \quad (6)$$

is also inverse first-order in ethylene concentration (eq 5). Finally, if β-H elimination by **K** is reversible and substitution of the unsaturated polymer chain of **L** by ethylene occurs by an associative mechanism (mechanism 4), the rate of chain transfer ($R_{transfer,4}$) is zero-order in ethylene concentration (eq 6). Mechanisms 1 and 4 are considered to be associative chain transfer processes because their rates are independent of ethylene concentration, and mechanisms 2 and 3 are considered to be dissociative chain transfer processes because their rates are inverse first-order in ethylene concentration.[3a,30]

The increase in MW with increasing ethylene pressure observed for ethylene polymerization by **5b**/**5b′** indicates that dissociative mechanisms 2 and/or 3 contribute to chain transfer in this system. A similar dependence of MW on ethylene pressure has been observed for (PO)PdR catalysts bearing bulky biaryl, menthyl, or *tert*-butyl substituents on the phosphine unit.[30] DFT computational studies showed that dissociative chain transfer mechanism 3 is competitive with associative chain transfer mechanism 4 for these sterically hindered catalysts, and this is probably the case for **5b**/**5b′** as well.

Additionally, the percentage of olefins that are internal (vs terminal) in the PE decreases from 60% to 15% as the ethylene pressure is raised from 410 to 850 psi. This result is consistent with a standard chain walking mechanism initiated by 2,1 insertion of intermediate **L** in Scheme 6.

Influence of $B(C_6F_5)_3$ on R_{growth} and $R_{transfer}$. The data in Table 1 show that the ethylene polymerization performance of (PPO)PdRL catalysts is significantly improved by the binding of $B(C_6F_5)_3$ to the PPO^- ligand. This section addresses this

DOI: 10.1021/acs.organomet.7b00815
Organometallics 2017, 36, 4990−5002

Table 3. Proportional Increases in R_{growth} and $R_{transfer}$ in (PPO)PdMeL Ethylene Polymerization Catalysts Resulting from Conversion of (PPO)PdRL to {PPO·B(C_6F_5)$_3$}PdRL Borane Adducts (Column I), Conversion of {PPO·B(C_6F_5)$_3$}PdRL to Base-Free {PPO·B(C_6F_5)$_3$}PdR Species (Column II), and Overall Conversion of (PPO)PdRL to {PPO·B(C_6F_5)$_3$}PdR Species (Column III), and Comparative Data for (PO)PdRL and (PO)Ni(allyl) Catalysts

		I		II		III	
		formation of B(C_6F_5)$_3$ adduct		formation of base-free species		formation of base-free B(C_6F_5)$_3$ adduct	
entry	complex	R_{growth}	$R_{transfer}$	R_{growth}	$R_{transfer}$	R_{growth}	$R_{transfer}$
1	**2a-lut**	50	8.6	5	5.8	250	50
2	**2b-lut**	14	6.6	6.7	6.1	88	48
3	**2c-lut**					250	130
4	**2d-py**					580	53
5	(*o*-P(3,5-^{t}Bu$_2$-Ph)$_2$-*p*-toluenesulfonate)PdMe(py)[a]	4.3	80				
6	(*o*-P(2-Et-Ph)$_2$-*p*-toluene-sulfonate)PdMe(py)[a,b]	3.6	42	5.3	3.4	19	140

[a]Conditions: 50 mL of toluene, 1.0 μmol of Pd, 435 psi ethylene, 80 °C, 1 h, ref 14. [b]Conditions: 50 mL of toluene, 2.0 μmol of Pd, 435 psi, 80 °C, 1 h, ref 19.

issue in more detail. The rates of chain growth (R_{growth}, R'_{growth}) and chain transfer ($R_{transfer}$, $R'_{transfer}$) for a pair of ethylene polymerization catalysts (cat, cat′) are related by eq 7, where X_n and X'_n are the corresponding number-average degrees of polymerization of the PE products. Here, we assume that growth rates are equal to activities. X_n data are obtained by GPC analysis ($X_n = M_n/28$). As summarized in Table 3, conversion of (PPO)PdRL species to {PPO·B(C_6F_5)$_3$}PdRL adducts results in large increases in R_{growth} and smaller increases in $R_{transfer}$ (column I, entries 1−4). Conversion of {PPO·B(C_6F_5)$_3$}PdRL species to base-free {PPO·B(C_6F_5)$_3$}PdR species further increases R_{growth} and $R_{transfer}$, in this case by a similar amount since the structure of the active {PPO·B(C_6F_5)$_3$}PdR(ethylene) species is not changed (column II). Overall, conversion of a (PPO)PdRL catalyst to a {PPO·B(C_6F_5)$_3$}PdR catalyst results in substantial increases in both R_{growth} (up to 580-fold) and the $R_{growth}/R_{transfer}$ ratio (up to 11-fold, column III).

$$\frac{R'_{transfer}}{R_{transfer}} = \frac{X_n R'_{growth}}{X'_n R_{growth}} \quad (7)$$

The allosteric binding of B(C_6F_5)$_3$ to (PPO)PdR complexes exerts a significant electronic effect on the catalytic site. B(C_6F_5)$_3$ coordination weakens the donor ability of the PPO$^-$ ligand and converts the neutral (PPO)PdMeL complex to a zwitterionic {PPO·B$^-$(C_6F_5)$_3$}Pd$^+$MeL species with increased positive charge at the Pd center.[31] The facile decoordination of 2,6-lutidine from **2a-lut** and **2b-lut** but not the corresponding B(C_6F_5)$_3$ adducts **3a-lut** and **3b-lut** in CD_2Cl_2 solution underscores the enhanced electrophilic character at Pd in the latter cases. On the basis of Mecking's studies of {P(2-OMe-4-X-Ph)$_2$benzenesulfonate}PdMe(dmso) ethylene polymerization catalysts, for which electron-withdrawing X substituents increase activity and decrease the PE MW,[2m] and studies of zwitterionic and cationic (PO)PdRL-type catalysts,[5,13,14,32] the increased charge at Pd in {PPO·B$^-$(C_6F_5)$_3$}Pd$^+$MeL species is expected to increase both R_{growth} and $R_{transfer}$, which is observed.

The steric effects of B(C_6F_5)$_3$ binding to (PPO)PdRL complexes are more subtle. Analysis of X-ray structures and SambVca plots[33] (see the Supporting Information) for the three sets of structurally characterized complexes—**2a-lut**/**3a-lut**, **2b-lut**/**3b-lut**/**5b′** and **2c-lut**/**5c**—shows that, in each case, the borane coordination results in a small increase in steric crowding of one axial face, a small decrease in steric crowding of the opposite axial face, and a small increase in lateral steric crowding,[34] but little change in the buried volume (%V_{bur}; see the Supporting Information). However, in the two structurally characterized pairs of catalysts for which the allosteric effect is most pronounced, **2a-lut**/**3a-lut** and **2c-lut**/**5c**, the B(C_6F_5)$_3$ "effector" induces significant changes in the conformation of the (PPO)Pd chelate rings and generates π-stacking interactions that may rigidify the structure and influence reactivity. The observation that conversion of **2b-py** to the {**1b**·B(C_6F_5)$_3$}PdR or {**1b**·BF_3}PdR species results in similar increases in R_{growth} (128- and 103-fold, respectively) and the $R_{growth}/R_{transfer}$ ratio (4.3- and 2.8-fold, respectively) for the two cases is consistent with a primarily electronic origin for these effects.[35] However, given that the $\Delta\Delta G^{\ddagger}$ values associated with these allosteric effects are quite small (<2 kcal mol^{-1}),[36] further studies will be required to explain their origin in more detail.

The large increase in R_{growth} and comparatively smaller increase in $R_{transfer}$ resulting from B(C_6F_5)$_3$ binding to (PPO)PdRL catalysts (Table 3, entries 1−4) contrasts with the smaller increase in R_{growth} and larger increase in $R_{transfer}$ observed for (PO)PdRL phosphine-sulfonate catalysts (entries 5, 6).[14,19] This difference has the important consequence that B(C_6F_5)$_3$ binding substantially increases both activity and PE MW for (PPO)PdRL catalysts, but only moderately increases activity and substantially *decreases* PE MW for (PO)PdRL catalysts. The smaller increase in $R_{transfer}$ upon B(C_6F_5)$_3$ binding to (PPO)PdRL catalysts vis-à-vis (PO)PdRL catalysts likely reflects the operation of a dissociative chain transfer mechanism in the former case, since the increased charge on Pd in the {PPO·B$^-$(C_6F_5)$_3$}Pd$^+$H(olefin) adduct **L** should inhibit olefin dissociation. Similar allosteric effects may be anticipated for other catalysts that undergo dissociative chain transfer.

CONCLUSION

Remote binding of B(C_6F_5)$_3$ to (PPO)PdMeL or {(PPO)-PdMe}$_2$ ethylene polymerization catalysts that contain phosphine-arenephosphinate or phosphine-arenephosphonate ligands significantly increases the catalyst activity and the molecular weight of the PE product. In the most favorable case, *in situ* conversion of (**1d**)PdMe(py) to the base-free adduct {**1d**·B(C_6F_5)$_3$}PdMe increases the ethylene polymerization activity from 9.8 to 5700 kg mol^{-1} h^{-1} and the M_n of the PE product from 9030 to 99 200 Da (80 °C, 410 psi). X-ray structural data, trends in ligand lability, and comparative studies of BF_3 activation suggest that these allosteric effects are

DOI: 10.1021/acs.organomet.7b00815
Organometallics 2017, 36, 4990−5002

primarily electronic in origin. The $B(C_6F_5)_3$ binding enhances R_{growth} by increasing the degree of positive charge on the Pd center. This effect does not result in the large increase in $R_{transfer}$ and concomitant reduction in PE molecular weight seen in previous studies of analogous (PO)PdRL catalysts that contain phosphine-arene*sulfonate* ligands, because of the operation of a dissociative chain transfer process, which is inhibited by the increased charge at Pd. This allosteric strategy for enhancing catalyst performance may be generally applicable to other catalysts that undergo dissociative chain transfer.

EXPERIMENTAL SECTION

General Procedures. All experiments were performed under a nitrogen atmosphere or vacuum using drybox or Schlenk techniques. Nitrogen was purified by passage over Q-5 oxygen scavenger and activated molecular sieves. Methylene chloride, diethyl ether, and THF were dried by passage over activated alumina. Pentane was purified by passage over BASF R3-11 oxygen scavenger and activated alumina. H[**1a**],[15,22] **4b**,[15] bis(2-methoxyphenyl)chlorophosphine,[15] and (TMEDA)$PdMe_2$[37] were prepared by literature procedures. $B(C_6F_5)_3$ was donated by Boulder Scientific.

NMR spectra were acquired on Bruker DRX-500 or DRX-400 spectrometers at ambient temperature unless otherwise indicated. ^1H and ^{13}C chemical shifts are reported relative to $SiMe_4$ and are internally referenced to residual ^1H and ^{13}C solvent resonances. ^{31}P and ^{19}F chemical shifts are reported relative to 85% H_3PO_4 and $CFCl_3$, respectively. Coupling constants are reported in Hz. Elemental analyses were performed by Robertson Microlit Laboratories. Residual solvent in elemental analysis samples was quantified by ^1H NMR. Mass spectrometry was performed on an Agilent 6224 TOF-MS instrument (high resolution) or an Agilent 6130 LC-MS (low resolution).

NMR Labeling Schemes. The labeling scheme of the carbons and hydrogens in the benzo-linker of the ligands are as shown in Chart 2.

Chart 2. Labeling Schemes for ^1H and ^{13}C NMR Spectra

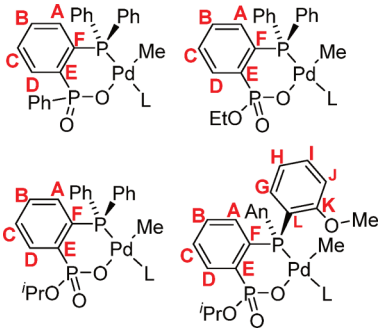

All other assignment labels are self-explanatory. NMR signals for ligands and complexes are assigned based on COSY, HMQC, HMBC, and $^1H\{^{31}P\}$ experiments, as well as trends in chemical shifts and coupling constants derived from these experiments.

1-PPh_2-2-P(O)(OEt)(OLi)-benzene (Li[1b]). A flask was charged with **4b** (3.25 g, 8.17 mmol), lithium bromide (1.20 g, 13.9 mmol), and acetonitrile (30 mL). The mixture was refluxed and stirred. A white solid began to precipitate after approximately 30 min. After ca. 40 h, the suspension was filtered and the white solid was washed with Et_2O (2 × 50 mL) and dried under vacuum (2.67 g, 82%). A minor impurity (15%) formed during the reaction and was identified as the ethylphosphonium zwitterion 1-P(Et)Ph_2-2-P(O)(OEt)(OLi)-benzene by ESI-MS, ^1H NMR, and $^{31}P\{^1H\}$ NMR. This material was not purified further but was used directly in the synthesis of H[**6a**]. $^{31}P\{^1H\}$ NMR (CD_3OD): δ 13.4 (s, *P*═O), −9.3 (s, *P*). ^1H NMR (CD_3OD): δ 8.07 (m, 1H, H^D), 7.37−7.22 (m, 12H), 7.08 (m, 1H, H^A), 3.55 (dq, $^3J_{HH} = {}^3J_{PH} = 7$, 2H, $-OCH_2CH_3$), 0.80 (t, $^3J_{HH} = 7$, 3H, $-OCH_2CH_3$). ESI-MS (CH_3OH, negative ion scan, *m*/*z*): 369.1 $[C_{20}H_{19}O_3P_2]^-$.

1-PPh_2-2-P(O)(O^{i}Pr)(OLi)-benzene (Li[1c]). A flask was charged with **4c** (1.50 g, 3.52 mmol) and acetonitrile (40 mL). The solution was saturated with LiBr at room temperature. The mixture was refluxed and stirred. A white solid began to precipitate after approximately 1 day. After ca. 10 days, the suspension was filtered, and the white solid was washed with acetonitrile (3 × 2 mL) and dried under vacuum (1.26 g, 88%). $^{31}P\{^1H\}$ NMR (CD_3OD): δ 12.2 (s, *P*═O), −9.3 (s, *P*). ^1H NMR (CD_2Cl_2): δ 8.09 (m, 1H, H^D), 7.34 (m, 1H, H^C), 7.26−7.21 (m, 11H, H^B, Ph−*H* signals), 7.09 (m, 1H, H^A), 4.48 (m, 1H, $-OCH(CH_3)_2$) 0.98 (d, $^3J_{HH}$ = 6.5, 6H, $-OCH(CH_3)_2$). $^{13}C\{^1H\}$ NMR (CD_3OD): δ 144.3 (dd, $^1J_{PC}$ = 178, $^2J_{PC}$ = 33.8, C^E), 141.2 (dd, $^1J_{PC}$ = 22.4, $^2J_{PC}$ = 11.5, C^F), 139.7 (d, $^3J_{PC}$ = 15, C^C), 136.9 (dd, $^2J_{PC}$ = 13.8, $^3J_{PC}$ = 2, C^A), 134.7 (d, $^2J_{PC}$ = 19.6, *o*-Ph), 134.3 (dd, $^2J_{PC} = {}^3J_{PC}$ = 9, C^D), 130.7 (d, $^3J_{PC}$ = 3, C^B), 129.1 (d, $^3J_{PC}$ = 6, *m*-Ph), 129.0 (d, $^1J_{PC}$ = 12.8, *ipso*-Ph), 129.0 (*p*-Ph), 69.0 (d, $^2J_{PC}$ = 5.9, $-OCH(CH_3)_2$), 24.5 (d, $^3J_{PC}$ = 4.3, $-OCH(CH_3)_2$). HRMS: calcd. for $[C_{21}H_{21}LiO_3P_2 - H_2O]^+$, *m*/*z* 372.10205. Found: 371.1003.

1-PAn_2-2-P(O)(O^{i}Pr)(OLi)-benzene (Li[1d]). A flask was charged with **4d** (1.50 g, 3.52 mmol) and acetonitrile (80 mL). The solution was saturated with LiBr at room temperature. The mixture was refluxed and stirred. After ca. 12 days, the volatiles were removed under vacuum. The solid was washed with CH_2Cl_2 and dried under vacuum. Because of similar solubility, Li[**1d**] and LiBr could not be separated and the mixture was used directly in the synthesis of H[**1d**]. $^{31}P\{^1H\}$ NMR (CD_3OD): δ 12.8 (s, *P*═O), −27.9 (s, *P*). ^1H NMR (CD_2Cl_2): δ 8.07 (m, 1H, H^D), 7.34 (m, H), 7.32 (t, H), 7.22 (t, 1H), 6.975(m, 2H), 6.93 (m, 1H), 6.78 (t, 2H, H^I), 6.54 (br, 2H, H^J), 4.46 (m, 1H, $-OCH(CH_3)_2$), 3.67 (s, 6H, $-OCH_3$), 0.99 (d, $^3J_{HH}$ = 6.5, 6H, $-OCH(CH_3)_2$). ESI-MS (CH_2Cl_2/MeOH 1:1 volume, pos. scan, *m*/*z*): 445.1 $[C_{23}H_{27}O_5P_2]^+$.

1-PPh_2-2-P(O)(OEt)(OH)-benzene (H[1b]). Li[**1b**] (1.70 g, 4.52 mmol) was suspended in distilled water (20 mL), and the mixture was acidified with HCl (2.3 mL, 4.6 mmol, 2.0 M in Et_2O). The mixture was extracted with CH_2Cl_2 (4 × 20 mL), and the solvent was removed under vacuum from the combined extracts to afford a white solid. The solid was recrystallized from THF/Et_2O at −40 °C (1.07 g, 64%). $^{31}P\{^1H\}$ NMR (CD_2Cl_2): δ 20.0 (s, *P*═O), −10.0 (s, *P*). ^1H NMR (CD_2Cl_2): δ 13.29 (s, 1H, −O*H*), 8.1 (m, 1H, H^D), 7.42−7.2 (m, 13H), 4.00 (dq, $^3J_{HH} = {}^3J_{PH}$ = 7, 2H, $-OCH_2CH_3$), 1.07 (t, $^3J_{HH}$ = 7.0, 3H, $-OCH_2CH_3$). $^{13}C\{^1H\}$ NMR (CD_2Cl_2): δ 141.2 (dd, $^1J_{PC}$ = 24, $^2J_{PC}$ = 13, C^F), 137.6 (d, $^1J_{PC}$ = 12.7, *ipso*-Ph), 135.9 (dd, $^2J_{PC}$ = 15, $^3J_{PC}$ = 2, C^A), 135.7 (dd, $^1J_{PC}$ = 195, $^2J_{PC}$ = 33, C^E), 134.0 (dd, $^2J_{PC} = {}^3J_{PC}$ = 9, C^D), 133.5 (d, $^2J_{PC}$ = 19.9, *o*-Ph), 132.0 (d, $^3J_{PC}$ = 3, C^B), 128.6 (d, $^3J_{PC}$ = 14.5, C^C), 128.4 (s, *p*-Ph), 128.3 (d, $^3J_{PC}$ = 6.5, *m*-Ph), 62.3 (d, $^2J_{PC}$ = 6, $-OCH_2CH_3$), 16.1 (d, $^3J_{PC}$ = 7, $-OCH_2CH_3$). ESI-MS (CH_2Cl_2/MeOH 1:1 volume, pos. scan, *m*/*z*): 371 $[M + H]^+$ HRMS: calcd. for $[C_{20}H_{21}O_3P_2]^+$ *m*/*z* 371.09661. Found: 371.0972.

1-PPh_2-2-P(O)(O^{i}Pr)(OH)-benzene (H[1c]). H[**1c**] was synthesized using a similar procedure to H[**1b**] with Li[**1c**] (0.35 g, 0.91 mmol), HCl (0.5 mL, 1.0 mmol, 2.0 M in Et_2O), and distilled water (15 mL). H[**1c**] was obtained as a white solid (0.24 g, 57%). $^{31}P\{^1H\}$ NMR (CD_2Cl_2): δ 18.7 (s, *P*═O), −10.6 (s, *P*). ^1H NMR (CD_2Cl_2): δ 12.08 (s, 1H, −O*H*), 8.02 (m, 1H, H^D), 7.40 (m, 1H, H^B), 7.35 (m, 1H, H^C), 7.32 (m, 6H, *p*-Ph and *o*-Ph), 7.22−7.18 (m, 5H, *m*-Ph and H^A), 4.75 (m, 1H, $-OCH(CH_3)_2$), 1.16 (d, $^3J_{HH}$ = 6.0, 6H, $-OCH(CH_3)_2$). $^{13}C\{^1H\}$ NMR (CD_2Cl_2): δ 141.3 (dd, $^1J_{PC}$ = 24.4, $^2J_{PC}$ = 13.7, C^F), 138.1 (d, $^1J_{PC}$ = 13, *ipso*-Ph), 136.4 (dd, $^1J_{PC}$ = 195, $^2J_{PC}$ = 32.7, C^E), 136.3 (d, $^2J_{PC}$ = 15.1, C^A), 133.8 (d, $^2J_{PC}$ = 19.5, *o*-Ph), 133.8 (dd, obscured by *o*-Ph, C^D), 132.2 (d, $^3J_{PC}$ = 4, C^B), 128.9 (d, $^3J_{PC}$ = 14.6, C^C), 128.7 (*p*-Ph), 128.7 (d, $^3J_{PC}$ = 6, *m*-Ph), 71.8 (d, $^2J_{PC}$ = 6.5, $-OCH(CH_3)_2$), 23.9 (d, $^3J_{PC}$ = 4.7, $-OCH(CH_3)_2$). HRMS: calcd. for $[C_{21}H_{22}O_3P_2]^+$ *m*/*z* 384.10443. Found: 384.1054. EA: Calcd for $C_{21}H_{22}O_3P_2 \cdot 0.007\ CH_2Cl_2$, %: C, 65.5; H, 5.77; N, 0. Found: C, 65.19; H, 5.68; N, <0.02.

1-PAn_2-2-P(O)(O^{i}Pr)(OH)-benzene (H[1d]). Li[**1d**] (1.02 g, 2.3 mmol), HCl (1.2 mL, 2.4 mmol, 2 M in Et_2O), and distilled water (75 mL). H[**1d**] was obtained as a white powder (0.585 g, 58%). $^{31}P\{^1H\}$

DOI: 10.1021/acs.organomet.7b00815
Organometallics 2017, 36, 4990−5002

NMR (CD_2Cl_2): δ 18.4 (s, P═O), −29.1 (s, P). ^{1}H NMR (CD_2Cl_2): δ 12.12 (s, 1H, −O*H*), 8.06 (m, 1H, H^D), 7.36 (m, 4H, H^H, H^B, H^C), 7.09 (m, 1H, H^A), 6.91 (m, 2H, H^G), 6.87 (t, 2H, H^I), 6.68 (t, 2H, H^J), 4.60 (m, 1H, −OC*H*(CH_3)$_2$), 3.66 (s, 6H, −OC*H*$_3$), 1.01 (d, $^3J_{HH}$ = 6, 6H, −OCH(C*H*$_3$)$_2$). ^{13}C{^{1}H} NMR (CD_2Cl_2): δ 161.4 (d, $^2J_{PC}$ = 14.3, C^K), 138.5 (br, C^F), 137.0 (dd, $^1J_{PC}$ = 191, $^2J_{PC}$ = 32.1, C^E), 135.8 (d, $^2J_{PC}$ = 15.1, C^A), 134.3 (s, C^J), 134.0 (dd, $^2J_{PC}$ = $^3J_{PC}$ = 10, C^D), 131.8 (C^B), 131.2 (C^H), 129.3 (d, $^3J_{PC}$ = 13.7, C^C), 123.3 (br, C^L), 121.4 (C^I), 110.9 (C^G), 71.1 (d, $^2J_{PC}$ = 6.3, −OC*H*(CH_3)$_2$), 56.0 (−OC*H*$_3$), 23.8 (d, $^3J_{PC}$ = 4.5, −OCH(C*H*$_3$)$_2$). ESI-MS (CH_2Cl_2/MeOH 1:1 volume, pos. scan, m/z): 445.2. HRMS: calcd. for $[C_{23}H_{27}O_5P_2]^+$, m/z 445.1334. Found: 445.1338.

(κ^2-*P*,*O*-1-PPh$_2$-2-PO$_2$Ph-Ph)PdMe(2,6-lutidine) (2a-lut). A vial was charged with H[**1a**] (0.191 g, 0.476 mmol) and (TMEDA)PdMe$_2$ (0.124 g, 0.491 mmol), and a solution of 2,6-lutidine (0.105 g, 0.980 mmol) in CH_2Cl_2 (8 mL) was added. The resulting clear solution was stirred for 7 h at room temperature. The volatiles were removed under vacuum to afford a white solid. The solid was suspended in Et_2O, collected by filtration, and dried under vacuum. The crude solid was found to contain 0.59 equiv of CH_2Cl_2 and 0.07 equiv of Et_2O (0.300 g, 92%). X-ray quality crystals of **2a-lut**·CH_2Cl_2 were grown from a CH_2Cl_2/THF solution that was cooled to −40 °C for ca. 10 weeks. As described in the text, dissolution of this compound in CD_2Cl_2 generated a mixture of **2a-lut**, free 2,6-lutidine, and a species formulated as the base-free species {(κ^2-1-*P*Ph$_2$-2-P*O*$_2$Ph-Ph)PdMe}$_n$, which partially precipitates from solution. Addition of excess 2,6-lutidine converts the base-free compound back to **2a-lut**. Data for **2a-lut**: ^{31}P{^{1}H} NMR (CD_2Cl_2): δ 31.4 (d, $^3J_{PP}$ = 14, *P*−Pd), 17.4 (d, $^3J_{PP}$ = 14, *P*═O). ^{1}H NMR (CD_2Cl_2), most aryl signals are multiplets that overlap with signals for free 2,6-lutidine and the base-free species; the following signals were resolved and identified as belonging to **2a-lut**: δ 7.87 (dddd, J = 11.9, 7.7, 3.8, 0.9, 1H), 7.63 (t, J = 7.6, 1H), 3.18 (s, 6H), −0.03 (d, $^3J_{PH}$ = 3.2, 3H, Pd−C*H*$_3$). Data for {(κ^2-1-*P*Ph$_2$-2-P*O*$_2$Ph-Ph)PdMe}$_n$: ^{31}P{^{1}H} NMR (CD_2Cl_2): δ 30.6 (br), δ 16.8 (br). ^{1}H NMR (CD_2Cl_2): δ 8.23 (m), 0.235 (d, $^3J_{PH}$ = 2.8, Pd−C*H*$_3$). HRMS: calcd. for $[C_{32}H_{32}O_2P_2NPd]^+$ m/z 630.09431. Found: 630.0919.

(κ^2-*P*,*O*-1-PPh$_2$-2-PO$_3$Et-Ph)PdMe(2,6-lutidine) (2b-lut). **2b-lut** was synthesized using a similar procedure to **2a-lut** with (TMEDA)PdMe$_2$ (0.147 g, 0.581 mmol), H[**1b**] (0.215 g, 0.581 mmol), 2,6-lutidine (0.12 mL, 1.0 mol), and CH_2Cl_2 (10 mL). **2b-lut** was obtained as a white solid (0.174 g, 44%). ^{31}P{^{1}H} NMR (CD_2Cl_2): 28.5 (d, $^3J_{PP}$ = 16, *P*═O), 9.4 (d, $^3J_{PP}$ = 17, *P*−Pd). ^{1}H NMR (CD_2Cl_2): 8.17 (m, 1H, H^D), 7.65 (t, $^3J_{HH}$ = 7, 1H, *p*-lut), 7.60 (m, 4H, *o*-Ph), 7.47 (m, 7H, H^C, *m*-Ph, and *p*-Ph), 7.34 (m, 1H, H^B), 7.18 (d, $^3J_{HH}$ = 8, 2H, *m*-lut), 7.03 (m, 1H, H^A), 3.15 (br, 8H, −OC*H*$_2$CH$_3$ and lut−C*H*$_3$), 0.56 (t, $^3J_{HH}$ = 7, 3H, −OCH$_2$C*H*$_3$), 0.04 (d, $^3J_{PH}$ = 3.0, 3H, Pd−C*H*$_3$). ^{13}C{^{1}H} NMR (CD_2Cl_2): δ 159.0 (*o*-lut), 143.2 (dd, $^1J_{PC}$ = 163, $^2J_{PC}$ = 19, C^E), 138.6 (*p*-lut), 135.2 (dd, J_{PC} = 21, 8, C^D), 134.7 (dd, $^2J_{PC}$ = 13, 3, C^A), 134.6 (d, $^2J_{PC}$= 12, *o*-Ph), 133.7 (dd, $^1J_{PC}$ = 46, $^2J_{PC}$ = 7, C^F), 131.5 (d, $^1J_{PC}$ = 53, *ipso*-Ph), 130.9 (d, $^4J_{PC}$ = 2, *p*-Ph), 130.3 (dd, J_{PC} = 15, 3, C^C), 129.7 (dd, J_{PC} = 20, 6, C^B), 128.9 (d, $^3J_{PC}$ = 11, *m*-Ph), 122.9 (d, $^4J_{PC}$ = 3, *m*-lut), 60.2 (d, $^2J_{PC}$ = 5, −OCH$_2$CH$_3$), 26.5 (lut−CH$_3$), 16.1 (d, $^3J_{PC}$ = 7, −OCH$_2$CH$_3$), −5.2 (d, $^2J_{PC}$ = 4, Pd−CH$_3$). ESI-MS (CH_2Cl_2/MeOH, 1:1 by volume, positive scan, m/z): 598.2 [MH]$^+$. HRMS: calcd. for $[C_{28}H_{32}P_2O_3NPd]^+$, m/z 598.0892. Found: 598.0897.

(κ^2-*P*,*O*-1-PPh$_2$-2-PO$_3$Et-Ph)PdMe(pyridine) (2b-py). **2b-py** was synthesized using a similar procedure to **2a-lut** with (TMEDA)PdMe$_2$ (0.055 g, 0.22 mmol), H[**1b**] (0.082 g, 0.22 mmol), pyridine (0.05 mL, 0.6 mmol), and CH_2Cl_2 (10 mL). **2b-py** was obtained as a pale yellow solid (0.040 g, 32%). ^{31}P{^{1}H} NMR ($CDCl_3$): 32.1 (d, $^3J_{PP}$ = 15, *P*═O), 10.4 (d, $^3J_{PP}$ = 15, *P*−Pd). ^{1}H NMR ($CDCl_3$): 8.85 (2H, *o*-py), 8.19 (m, 1H, H^D), 7.86 (t, $^3J_{HH}$ = 7, 1H, *p*-py), 7.58−7.38 (m, 13H, H^C, *m*-py, Ph signals), 7.34 (td, $^3J_{HH}$ = 7.6, 1.4, 1H, H^B), 7.02 (m, 1H, H^A), 3.35 (dq, $^3J_{HH}$ = $^3J_{PH}$ = 7, 2H, −OC*H*$_2$CH$_3$), 0.66 (t, $^3J_{HH}$ = 7, 3H, −OCH$_2$C*H*$_3$), 0.28 (d, $^3J_{PH}$ = 2.5, 3H, Pd−C*H*$_3$). ^{13}C{^{1}H} NMR (CD_2Cl_2): δ 150.5 (*o*-py), 138.6 (*p*-py), 135.3 (d, $^2J_{PC}$ = 10.3, C^D), 134.8 (obscured by *o*-Ph, C^A), 134.7 (d, $^2J_{PC}$= 12, *o*-Ph), 133.4 (C^F), 131.4 (*ipso*-Ph), 131.0 (*p*-Ph), 130.4 (C^C), 129.7 (C^B), 128.9 (d, $^3J_{PC}$ = 10.6, *m*-Ph), 125.3 (*m*-py), 60.1 (−OCH$_2$CH$_3$), 16.1 (d, $^3J_{PC}$ = 8, −OCH$_2$CH$_3$), 0.7 (Pd−CH$_3$), C^E not observed. HRMS: calcd. for $[C_{26}H_{28}P_2O_3NPd]^+$, m/z 570.0579. Found: 570.0563.

(κ^2-*P*,*O*-1-PPh$_2$-2-PO$_3$^{i}Pr-Ph)PdMe(2,6-lutidine) (2c-lut). **2c-lut** was synthesized using a similar procedure to **2a-lut** with (TMEDA)PdMe$_2$ (0.079 g, 0.313 mmol), H[**1c**] (0.120 g, 0.313 mmol), 2,6-lutidine (0.04 mL, 0.313 mmol), and CH_2Cl_2 (10 mL). **2c-lut** was obtained as a white solid (0.068 g, 36%). ^{31}P{^{1}H} NMR (CD_2Cl_2): δ 28.7 (d, $^3J_{PP}$ = 16, *P*═O), 7.8 (d, $^3J_{PP}$ = 17, *P*−Pd). ^{1}H NMR (CD_2Cl_2): δ 8.17 (m, 1H, H^D), 7.65 (m, 4H, *o*-Ph), 7.55 (br t, 1H, *p*-lut), 7.47 (m, 6H, *m*-Ph, *p*-Ph), 7.42 (m, 1H, H^C), 7.33 (t, $^3J_{HH}$ = 7.5, 1H, H^B), 7.20 (d, $^3J_{HH}$ = 8, 2H, *m*-lut), 7.08 (m, 1H, H^A), 4.21 (m, 1H, −OC*H*(CH_3)$_2$), 3.16 (s, 6H, lut−C*H*$_3$), 0.56 (d, $^3J_{HH}$ = 5.5, 6H, −OCH(C*H*$_3$)$_2$), −0.05 (d, $^3J_{PH}$ = 2.5, 3H, Pd−C*H*$_3$). ^{13}C{^{1}H} NMR (CD_2Cl_2): δ 158.9 (*o*-lut), 144.8 (dd, $^1J_{PC}$ = 165, $^2J_{PC}$ = 19, C^E), 138.6 (*p*-py), C^D obscured by *o*-Ph, 134.7 (d, $^2J_{PC}$ = 12, *o*-Ph), 134.4 (dd, J_{PC} = 11, 7.8, C^A), 133.5 (dd, $^1J_{PC}$ = 45.7, $^2J_{PC}$ = 6.5, C^F), 131.4 (d, $^1J_{PC}$ = 53.2, *ipso*-Ph), 130.8 (d, $^4J_{PC}$ = 2.4, *p*-Ph), 130.4 (dd, J_{PC} = 12, 2.4, C^C), 129.3 (dd, J_{PC} = 7, 2.4, C^B), 128.8 (d, $^3J_{PC}$ = 10.9, *m*-Ph), 122.8, (*m*-lut), 68.6 (d, $^2J_{PC}$ = 5.8, −OCH(CH_3)$_2$), 26.5 (lut−CH$_3$), 23.5 (d, $^3J_{PC}$ = 4, −OCH(CH_3)$_2$), −5.2 (d, $^2J_{PC}$ = 4, Pd−CH$_3$). HRMS calc. for $[C_{29}H_{34}NO_3P_2Pd]^+$ m/z 612.10488. Found: 612.1036.

(κ^2-*P*,*O*-1-PPh$_2$-2-PO$_3$^{i}Pr-Ph)PdMe(pyridine) (2c-py). **2c-py** was synthesized using a similar procedure to **2a-lut** with (TMEDA)PdMe$_2$ (0.139 g, 0.552 mmol), H[**1c**] (0.212 g, 0.552 mmol), pyridine (0.09 mL, 1.12 mmol), and CH_2Cl_2 (10 mL). **2c-py** was obtained as an off-white solid (0.128 g, 40%). ^{31}P{^{1}H} NMR (CD_2Cl_2): δ 32.4 (d, $^3J_{PP}$ = 14, *P*═O), 8.6 (d, $^3J_{PP}$ = 14, *P*−Pd). ^{1}H NMR (CD_2Cl_2): δ 8.87 (d, $^3J_{HH}$ = 4, 2H, *o*-py), 8.20 (m, 1H, H^D), 7.87 (br t, $^3J_{HH}$ = 7.5, 1H, *p*-py), 7.60 (m, $^3J_{HH}$ = 7, 4H, *o*-Ph), 7.5−7.42 (m, 9H, H^C, *m*-py, *m*-Ph, *p*-Ph), 7.31 (t, $^3J_{HH}$ = 7.5, 1H, H^B), 7.05 (m, 1H, H^A), 4.23 (m, 1H, −OC*H*(CH_3)$_2$) 0.70 (d, $^3J_{HH}$ = 6.0, 6H, −OCH(C*H*$_3$)$_2$), 0.25 (d, $^3J_{PH}$ = 2, 3H, Pd−C*H*$_3$). ^{13}C{^{1}H} NMR (CD_2Cl_2): δ 150.5 (*o*-py), 144.1 (dd, $^1J_{PC}$ = 168, $^2J_{PC}$ = 19, C^E), 138.4 (*p*-py), C^D obscured by *o*-Ph and C^A, 134.7 (d, $^2J_{PC}$ = 12, *o*-Ph), 134.6 (dd, J_{PC} = 3.1, 10.3, C^A), 132.8 (d, $^1J_{PC}$ = 44.1, C^F), 131.3 (d, $^1J_{PC}$ = 53.3, *ipso*-Ph), 130.9 (d, $^4J_{PC}$ = 2.1, *p*-Ph), 130.5 (dd, J_{PC} = 11, 4, C^C), 129.5 (dd, J_{PC} = 7.2, 2.3, C^B), 128.8 (d, $^3J_{PC}$ = 10.9, *m*-Ph), 125.2, (*m*-py), 68.3 (d, $^2J_{PC}$ = 5.5, −OCH(CH_3)$_2$), 23.9 (d, $^3J_{PC}$ = 4, −OCH(CH_3)$_2$), 0.6 (Pd−CH$_3$). HRMS calc. for $[C_{27}H_{30}NO_3P_2Pd]^+$ m/z 584.07358. Found: 584.0724.

(κ^2-*P*,*O*-1-PAn$_2$-2-PO$_3$^{i}Pr-Ph)PdMe(pyridine) (2d-py). **2d-py** was synthesized using a similar procedure to **2a-lut** with (TMEDA)PdMe$_2$ (0.118 g, 0.465 mmol), H[**1d**] (0.206 g, 0.464 mmol), pyridine (80 μL, 0.99 mmol), and CH_2Cl_2 (10 mL). **2d-py** was obtained as an off-white solid (0.161 g, 54%). ^{31}P{^{1}H} NMR (CD_2Cl_2): δ 24.6 (br, *P*═O), 9.1 (d, $^3J_{PP}$ = 11.9, *P*−Pd). ^{1}H NMR (CD_2Cl_2): δ 8.89 (d, $^3J_{HH}$ = 3.0, 2H, *o*-py), 8.10 (m, 1H, H^D), 7.84 (t, $^3J_{HH}$ = 7.5, 1H, *p*-py), 7.52 (t, $^3J_{HH}$ = 7.5, 2H, H^H), 7.46−7.41 (m, 5H, m-py, H^J, H^C), 7.23 (t, $^3J_{HH}$ = 7.0, 1H, H^B), 7.19 (m, 1H, H^A), 6.97 (m, 2H, H^I and H^G), 4.15 (m, 1H, −OC*H*(CH_3)$_2$), 3.65 (s, 6H, −OC*H*$_3$), 0.73 (d, $^3J_{HH}$ = 5.0, 6H, −OCH(C*H*$_3$)$_2$), 0.12 (d, $^3J_{PH}$ = 2.5, 3H, Pd−C*H*$_3$). ^{13}C{^{1}H} NMR (CD_2Cl_2): δ 161.1 (d, $^2J_{PC}$ = 3.1, C^K), 150.8 (*o*-py), 143.4 (dd, $^1J_{PC}$ = 165, $^2J_{PC}$ = 20.1, C^E), 138.2 (*p*-py), 137.1 (br, C^J), 134.3 (dd, J_{PC} = 18.7, 7.7, C^D), 134.0 (d, $^2J_{PC}$ = 8.4, C^A), 133.2 (C^H), 131.8 (dd, $^1J_{PC}$ = 52, $^2J_{PC}$ = 8.3, C^F), 129.7 (d, $^3J_{PC}$ = 12.1, C^C), 128.3 (d, $^3J_{PC}$ = 7.0, C^B), 125.1 (*m*-py), 120.9 (d, $^2J_{PC}$ = 10.7, C^G), 118.7 (d, $^1J_{PC}$ = 54, C^L), 111.7 (d, $^4J_{PC}$ = 4.4, C^I), 67.8 (d, $^2J_{PC}$ = 5.5, −OCH(CH_3)$_2$), 55.6 (−OCH$_3$), 23.9 (d, $^3J_{PC}$ = 3.3, −OCH(CH_3)$_2$), 0.31 (Pd−CH$_3$). HRMS calc. for $[C_{29}H_{34}NO_5P_2Pd]^+$ m/z 644.09472. Found: 644.0936.

(κ^2-1-*P*Ph$_2$-2-P(*O*)(O-B(C$_6$F$_5$)$_3$)Ph-Ph)PdMe(2,6-lutidine) (3a-lut). A vial was charged with **2a-lut** (0.203 g, 0.296 mmol), B(C_6F_5)$_3$ (0.184 g, 0.359 mmol), and CH_2Cl_2 (3 mL). The resulting yellow solution was stirred in the dark at room temperature for 1 h. The stirring was terminated, pentane was layered onto the CH_2Cl_2, and the mixture was stored at −40 °C for 20 h, after which a white solid had formed. The solid was collected, rinsed with pentane, and dried under vacuum. The crude solid was purified by Soxhlet extraction into cyclohexane, washed with hexanes, and dissolved in minimum CH_2Cl_2. Hexanes was added to precipitate **3a-lut** as a white solid, which was

DOI: 10.1021/acs.organomet.7b00815
Organometallics 2017, 36, 4990−5002

found by ^{1}H NMR to contain 0.15 equiv of CH_2Cl_2 and 0.074 equiv of hexanes (0.720 g, 21%). X-ray quality crystals of **3a-lut** were grown by layering hexanes onto a CH_2Cl_2 solution of **3a-lut**. $^{31}P\{^1H\}$ NMR (CD_2Cl_2): δ 31.1 (d, $^3J_{PP}$ = 17, *P*–Pd), 22.7 (d, $^3J_{PP}$ = 17, *P*═O). ^{1}H NMR (CD_2Cl_2): δ 8.44 (dddd, $^3J_{PH}$ = 12.1, $^4J_{PH}$ = 3.9, $^3J_{HH}$ = 7.8, $^4J_{HH}$ = 0.9, 1H, H^D), 7.67 (t, $^3J_{HH}$ = 7.6, 1H, *p*-lut), 7.62 (td, $^3J_{HH}$ = 7.6, $^4J_{HH}$ = 0.8, H^B), 7.53–7.37 (m, 4H, H^C and 3 Ph–*H*), 7.31 (tq, $^3J_{HH}$ = 7.0, $^4J_{HH}$ = 1.8, $^5J_{PH}$ = 1.8, 1H, Ph–*H*), 7.24 (d, $^3J_{HH}$ = 7.8, 1H, *m*-lut), 7.24–7.10 (m, 6H, Ph–*H*), 7.08 (d, $^3J_{HH}$ = 8.2, 1H, *m*-lut), 7.10–7.02 (m, 3H, Ph–*H*), 6.99 (ddd, $^3J_{HH}$ = 8, J_{PH} = 9.5, 5.7, 1H, H^A), 6.84 (td, $^3J_{HH}$ = 7.8, J_{PH} = 3.7, 2H, Ph-*H*), 3.08 (s, 3H, lut–CH_3), 2.96 (s, 3H, lut–CH_3), 0.13 (d, $^3J_{PH}$ = 3.5, 3H, Pd–CH_3). $^{13}C\{^1H\}$ (CD_2Cl_2): δ 158.9 (d, $^3J_{PC}$ = 1, *o*-lut), 158.2 (d, $^3J_{PC}$ = 1, *o*-lut), 148.1 (dm, $^1J_{FC}$ = 240, *o*-C_6F_5), 139.6 (dd, $^1J_{PC}$ = 136, $^2J_{PC}$ = 17, C^E), 139.2 (dm, $^1J_{FC}$ = 246, *p*-C_6F_5), 139.0 (*p*-lut), 136.8 (ddd, $^1J_{FC}$ = 246, $^2J_{FC}$ = 21, $^2J_{FC}$ = 12, *m*-C_6F_5), 136.0 (dd, J_{PC} = 11, 3, C^A), 135.2 (t, J_{PC} = 9), 134.5 (d, J_{PC} = 13), 133.7 (d, J_{PC} = 11), 133.0 (d, J_{PC} = 45), 131.9 (dd, $^1J_{PC}$ = 44, $^2J_{PC}$ = 12, C^F), 131.7 (d, J_{PC} = 3), 131.5 (dd, J_{PC} = 7, 3, C^C), 131.2 (d, J_{PC} = 3), 131.1 (d, J_{PC} = 3), 131.0 (dd, J_{PC} = 11, 2, C^B), 130.9 (d, J_{PC} = 11), 130.8 (d, J_{PC} = 56), 129.3 (d, J_{PC} = 11), 129.1 (d, J_{PC} = 11), 127.6 (d, J_{PC} = 14), 127.4 (d, J_{PC} = 49), 123.1 (d, $^4J_{PC}$ = 3, *m*-lut), 122.6 (d, $^4J_{PC}$ = 3, *m*-lut), 122.0 (br s, *ipso*-C_6F_5), 26.6 (lut–CH_3), 26.0 (lut–CH_3), −2.7 (t, $^2J_{PC}$ = 3, Pd–CH_3). Unassigned $^{13}C\{^1H\}$ signals are Ph–*C* resonances. $^{19}F\{^1H\}$ NMR (CD_2Cl_2): δ −133.1 (d, $^3J_{FF}$ = 20.8, *o*-C_6F_5), −161.4 (t, $^3J_{FF}$ = 20.8, *p*-C_6F_5), −166.7 (br t, $^3J_{FF}$ = 19.1, *m*-C_6F_5). ^{11}B NMR (CD_2Cl_2): δ −2.5. EA: Calcd for $C_{50}H_{31}NO_2BF_{15}P_2Pd\cdot0.145\ CH_2Cl_2\cdot0.074\ C_6H_{14}$, %: C, 52.36; H, 2.82; N, 1.20. Found: C, 52.04; H, 3.01; N, 1.16.

(κ^2-*P*,*O*-1-PPh_2-2-PO_2Et(O-B(C_6F_5)$_3$-Ph)PdMe(2,6-lutidine) (3b-lut). **3b-lut** was synthesized using a similar procedure to **3a-lut** with **2b-lut** (0.150 g, 0.248 mmol), B(C_6F_5)$_3$ (0.127 g, 0.250 mmol), and CH_2Cl_2 (5 mL). **3b-lut** was obtained as a white solid (0.812 g, 29%). $^{31}P\{^1H\}$ NMR (CD_2Cl_2): δ 29.6 (d, $^3J_{PP}$ = 18, *P*═O), 9.8 (d, $^3J_{PP}$ = 18, *P*–Pd). ^{1}H NMR (CD_2Cl_2): δ 8.01 (m 1H, H^D), 7.67 (m, 3H, *p*-lut and *o*-Ph), 7.58–7.44 (m, 8H, H^B, H^C, *m*-Ph and *p*-Ph), 7.34 (dd, $^3J_{HH}$ = 7.5, 2H, *o*-Ph), 7.21 (d, $^3J_{HH}$ = 8.0, 1H, *m*-lut), 7.14 (dd, $^3J_{HH}$ = $^3J_{PH}$ = 7.0, 1H, H^A), 7.10 (d, $^3J_{HH}$ = 8.0, 1H, *m*-lut), 3.49 (m, 1H, −OCH_2CH$_3$), 3.00 (s, 3H, lut–CH_3), 2.86 (s, 3H, lut–CH_3), 2.85 (m, 1H, −OCH_2CH$_3$) 0.41 (t, $^3J_{HH}$ = 7, 3H, −OCH$_2$CH_3), 0.06 (d, $^3J_{PH}$ = 3.5, 3H, Pd–CH_3). $^{13}C\{^1H\}$ NMR (CD_2Cl_2): δ 158.6 (*o*-lut), 158.4 (*o*-lut), 148.4 (dm, $^1J_{FC}$ = 240, *o*-C_6F_5), 139.3 (d, $^1J_{FC}$ = 247, *p*-C_6F_5), 139.0 (*p*-lut), 137.0 (d, $^1J_{FC}$ = 258, *m*-C_6F_5), 135.8 (dd, $^1J_{PC}$ = 192, $^2J_{PC}$ = 16.7, C^E), 135.6 (dd, J_{PC} = 13, 2.4, C^A), 135.1 (d, $^2J_{PC}$ = 13, *o*-Ph), 135.0 (m, C^D), 134.0 (d, $^2J_{PC}$ = 10.7, C^F, partially obscured by *o*-Ph), 133.7 (d, $^2J_{FC}$ = 12, *o*-Ph), 132.1 (d, $^4J_{PC}$ = 2.5, *p*-Ph), 131.7 (dd, J_{PC} = 6.8, 2.8, C^C), 131.1 (d, $^4J_{PC}$ = 2.4, *p*-Ph), 130.9 (d, $^1J_{PC}$ = 56, *ipso*-Ph), 130.7 (dd, J_{PC} = 13, 2.3, C^B), 129.5 (d, $^3J_{PC}$ = 10.9, *m*-Ph), 129.1 (d, $^3J_{PC}$ = 10.7, *m*-Ph), 128.9 (d, $^1J_{PC}$ = 52, *ipso*-Ph), 123.0 (d, $^4J_{PC}$ = 3.1, *m*-lut), 122.6 (d, $^4J_{PC}$ = 3.3, *m*-lut), 121.7 (br s, *ipso*-C_6F_5), 62.5 (d, $^2J_{PC}$ = 5.3, −OCH$_2$CH$_3$), 26.1 (s, lut–CH_3), 25.8 (s, lut–CH_3), 14.9 (d, $^3J_{PC}$ = 8.8, −OCH$_2$CH_3), −3.2 (Pd–CH_3). $^{19}F\{^1H\}$ NMR (CD_2Cl_2): δ −134.0 (d, $^3J_{FF}$ = 22.1, *o*-C_6F_5), −161.2 (t, $^3J_{FF}$ = 20.7, *p*-C_6F_5), −166.9 (t, $^3J_{FF}$ = 20.7, *m*-C_6F_5). ^{11}B NMR (CD_2Cl_2): δ −2.3. HRMS: calcd. for $[C_{46}H_{31}BF_{15}NO_3P_2Pd]^+$, *m*/*z* 1109.06672. Found: 1109.067.

{(κ^2-*P*,*O*-1-PPh_2-2-PO_2Et(O-B(C_6F_5)$_3$-Ph)PdMe}$_2$, (5b/5b′). A vial was charged with **2b-py** (0.201 g, 0.351 mmol), B(C_6F_5)$_3$ (0.360 g, 0.704 mmol), and CH_2Cl_2 (7 mL), and the mixture was stirred for 1 h, resulting in a bright yellow solution. The mixture was concentrated, layered with hexanes, and stored at −40 °C for 48 h, and a white solid precipitated. The solid was collected by filtration and recrystallized again from a CH_2Cl_2/hexanes solution at −40 °C. X-ray quality crystals were grown from $C_2H_2Cl_4$/hexanes solution at room temperature (0.184 g, 52%). **5b**. $^{31}P\{^1H\}$ NMR (CD_2Cl_2): δ 37.3 (br, *P*═O), 11.3 (br, *P*–Pd). ^{1}H NMR (CD_2Cl_2): δ 7.8 (br, 1H, H^D), 7.6–7.23 (br, 12H, *H*–Ph), 6.93 (br, 1H, H^A), 4.45 (br, 2H, −OCH_2CH$_3$), 3.7 (br, 2H, −OCH_2CH$_3$), 0.71 (br t, 6H, −OCH$_2$CH_3) −0.03 (br d, 6H, Pd–CH_3). $^{19}F\{^1H\}$ NMR (CD_2Cl_2): δ −133.0 (br, *o*-C_6F_5), −159.5 (br, *p*-C_6F_5), −165.7 (br, *m*-C_6F_5). **5b′**. $^{31}P\{^1H\}$ NMR (CD_2Cl_2): δ 37.0 (br, *P*═O), 9.7 (br, *P*–Pd). ^{1}H NMR (CD_2Cl_2): δ 7.90 (br, 1H, H^D), 7.6–7.3 (br, 12H, *H*–Ph), 7.13, (br, 1H, H^A), 3.63 (br, 2H, −OCH_2CH$_3$), 2.99 (br, 2H, −OCH_2CH$_3$), 0.51 (br, 6H, −OCH$_2$CH$_3$), 0.40 (br, 6H, Pd–CH_3). $^{19}F\{^1H\}$ NMR (CD_2Cl_2): δ −133.7 (br, *o*-C_6F_5), −160.8 (br, *p*-C_6F_5), −166.3 (br, *m*-C_6F_5). $^{13}C\{^1H\}$ and ^{11}B NMR too broad to make assignments. HRMS: calcd. for $[C_{78}H_{44}B_2F_{30}O_6P_4Pd_2 + 2Na]^{2+}$ *m*/*z* 2005.990218. Found: 2005.9978.

{(κ^2-*P*,*O*-1-PPh_2-2-$PO_2{}^i$Pr(O-B(C_6F_5)$_3$-Ph)PdMe}$_2$ (5c). **5c** was synthesized using a similar procedure to **5b**/**5b′** with **2c-py** (0.104 g, 0.178 mmol), B(C_6F_5)$_3$ (0.182 g, 0.356 mmol), and CH_2Cl_2 (5 mL). **5c** was obtained as a white solid (0.100 g, 87%). $^{31}P\{^1H\}$ NMR (CD_2Cl_2): δ 36.6 (br d, *P*═O), 6.1 (d, $^3J_{PP}$ = 13.4, *P*–Pd). ^{1}H NMR (CD_2Cl_2): δ 7.69 (m, 1H, H^D), 7.6–7.36 (m, 12H, *H*–Ph), 7.13 (m, 1H, H^A), 4.36 (m, 1H, −OCH(CH$_3$)$_2$), 0.93 (d, $^3J_{HH}$ = 6.0, 6H, −OCH(CH_3)$_2$), 0.67 (br d, $^3J_{HH}$ = 5, 6H, −OCH(CH_3)$_2$), 0.35 (br, 6H, Pd–CH_3). $^{19}F\{^1H\}$ NMR (CD_2Cl_2): δ −134.2 (d, $^3J_{FF}$ = 19, *o*-C_6F_5), −161.7 (t, $^3J_{FF}$ = 20, *p*-C_6F_5), −167.0 (t, $^3J_{FF}$ = 17, *m*-C_6F_5). $^{13}C\{^1H\}$ and ^{11}B NMR too broad to make assignments. HRMS calc. for $[C_{80}H_{49}B_2F_{30}O_6P_4Pd_2 - H_2O]^+$ *m*/*z* 2017.0154. Found: 2017.0201.

Ethylene Polymerization Procedure. Polymerization reactions were run in a stainless steel Parr 300 mL autoclave, which was equipped with a mechanical stirrer, thermocouple, water cooling loop, and a Parr 4842 controller. In a glovebox, the catalyst was weighed directly into a 200 mL glass autoclave liner. When applicable, B(C_6F_5)$_3$ was also weighed directly into the liner. Toluene (50 mL) was added, and the liner was placed in a stainless steel autoclave, which was sealed and removed from the glovebox. The autoclave was heated to 80 °C and pressurized with ethylene while the contents were stirred. After 2 h, the autoclave was cooled to 25 °C and vented. Acetone (50 mL) was added to precipitate the polymer. The polymer was collected by filtration, rinsed with acetone, and dried overnight in a vacuum oven. The oligomer content of the filtrate was determined by GC–MS and ^{1}H NMR analysis. For polymerizations with B(C_6F_5)$_3$·Et_2O and BF_3·Et_2O, the catalyst and activator were injected in a 10 mL toluene solution after the autoclave was heated and pressurized with ethylene.

■ ASSOCIATED CONTENT

Supporting Information

The Supporting Information is available free of charge on the ACS Publications website at DOI: 10.1021/acs.organomet.7b00815.

Additional experimental procedures, NMR data for compounds, supporting tables, kinetic derivations (PDF)

Accession Codes

CCDC 1562320–1562326 contain the supplementary crystallographic data for this paper. These data can be obtained free of charge via www.ccdc.cam.ac.uk/data_request/cif, or by emailing data_request@ccdc.cam.ac.uk, or by contacting The Cambridge Crystallographic Data Centre, 12 Union Road, Cambridge CB2 1EZ, UK; fax: +44 1223 336033.

■ AUTHOR INFORMATION

Corresponding Author

*E-mail: rfjordan@uchicago.edu.

ORCID

Alison M. Johnson: 0000-0002-7297-5400

Richard F. Jordan: 0000-0002-3158-4745

Author Contributions

The manuscript was written through contributions of all authors.

DOI: 10.1021/acs.organomet.7b00815
Organometallics 2017, 36, 4990–5002

Funding

This work was supported by National Science Foundation grants CHE-0911180 and CHE-1709159.

Notes

The authors declare no competing financial interest.

■ ACKNOWLEDGMENTS

The authors thank Antoni Jurkiewicz and Chang-Jin Qin for assistance with NMR spectroscopy and mass spectrometry, respectively, and Ian Steele and Alexander Filatov for assistance with X-ray crystallography.

■ REFERENCES

(1) (a) Nakamura, A.; Ito, S.; Nozaki, K. *Chem. Rev.* **2009**, *109*, 5215−5244. (b) Nakamura, A.; Anselment, T. M.; Claverie, J.; Goodall, B.; Jordan, R. F.; Mecking, S.; Rieger, B.; Sen, A.; van Leeuwen, P. W.; Nozaki, K. *Acc. Chem. Res.* **2013**, *46*, 1438−1449. (c) Ito, S.; Nozaki, K. *Chem. Rec.* **2010**, *10*, 315−325.

(2) (a) Drent, E.; van Dijk, R.; van Ginkel, R.; van Oort, B.; Pugh, R. I. *Chem. Commun.* **2002**, 744−745. (b) Guironnet, D.; Roesle, P.; Runzi, T.; Gottker-Schnetmann, I.; Mecking, S. *J. Am. Chem. Soc.* **2009**, *131*, 422−423. (c) Kochi, T.; Noda, S.; Yoshimura, K.; Nozaki, K. *J. Am. Chem. Soc.* **2007**, *129*, 8948−8949. (d) Luo, S.; Vela, J.; Lief, G. R.; Jordan, R. F. *J. Am. Chem. Soc.* **2007**, *129*, 8946−8947. (e) Ito, S.; Munakata, K.; Nakamura, A.; Nozaki, K. *J. Am. Chem. Soc.* **2009**, *131*, 14606−14607. (f) Weng, W.; Shen, Z.; Jordan, R. F. *J. Am. Chem. Soc.* **2007**, *129*, 15450−15451. (g) Leicht, H.; Gottker-Schnetmann, I.; Mecking, S. *Angew. Chem., Int. Ed.* **2013**, *52*, 3963−3966. (h) Borkar, S.; Newsham, D. K.; Sen, A. *Organometallics* **2008**, *27*, 3331−3334. (i) Skupov, K. M.; Piche, L.; Claverie, J. P. *Macromolecules* **2008**, *41*, 2309−2310. (j) Ota, Y.; Ito, S.; Kuroda, J.; Okumura, Y.; Nozaki, K. *J. Am. Chem. Soc.* **2014**, *136*, 11898−11901. (k) Jian, Z.; Wucher, P.; Mecking, S. *Organometallics* **2014**, *33*, 2879−2888. (l) Contrella, N. D.; Jordan, R. F. *Organometallics* **2014**, *33*, 7199−7208. (m) Wucher, P.; Goldbach, V.; Mecking, S. *Organometallics* **2013**, *32*, 4516−4522. (n) Neuwald, B.; Falivene, L.; Caporaso, L.; Cavallo, L.; Mecking, S. *Chem.—Eur. J.* **2013**, *19*, 17773−17788. (o) Piche, L.; Daigle, J. C.; Rehse, G.; Claverie, J. P. *Chem.—Eur. J.* **2012**, *18*, 3277−3285. (p) Skupov, K. M.; Marella, P. R.; Simard, M.; Yap, G. P. A.; Allen, N.; Conner, D.; Goodall, B. L.; Claverie, J. P. *Macromol. Rapid Commun.* **2007**, *28*, 2033−2038. (q) Wu, Z.; Chen, M.; Chen, C. *Organometallics* **2016**, *35*, 1472−1479. (r) Wada, S.; Jordan, R. F. *Angew. Chem.* **2017**, *129*, 1846−1824. (s) Gaikwad, S. R.; Deshmukh, S. S.; Gonnade, R. G.; Rajamohanan, P. R.; Chikkali, S. H. *ACS Macro Lett.* **2015**, *4*, 933−937.

(3) (a) Noda, S.; Nakamura, A.; Kochi, T.; Chung, L. W.; Morokuma, K.; Nozaki, K. *J. Am. Chem. Soc.* **2009**, *131*, 14088−14100. (b) Haras, A.; Anderson, G. D. W.; Michalak, A.; Rieger, B.; Ziegler, T. *Organometallics* **2006**, *25*, 4491−4497. (c) Nozaki, K.; Kusumoto, S.; Noda, S.; Kochi, T.; Chung, L. W.; Morokuma, K. *J. Am. Chem. Soc.* **2010**, *132*, 16030−16042.

(4) (a) Britovsek, G. J. P.; Gibson, V. C.; Wass, D. F. *Angew. Chem., Int. Ed.* **1999**, *38*, 428−447. (b) Gibson, V. C.; Spitzmesser, S. K. *Chem. Rev.* **2003**, *103*, 283. (c) Ittel, S. D.; Johnson, L. K.; Brookhart, M. *Chem. Rev.* **2000**, *100*, 1169−1204. (d) Camacho, D. H.; Guan, Z. *Chem. Commun.* **2010**, *46*, 7879−7893. (e) Franssen, N. M. G.; Reek, J. N. H.; de Bruin, B. *Chem. Soc. Rev.* **2013**, *42*, 5809−5832. (f) Mu, H.; Pan, L.; Song, D.; Li, Y. *Chem. Rev.* **2015**, *115*, 12091−12137.

(5) (a) Kim, Y.; Jordan, R. F. *Organometallics* **2011**, *30*, 4250−4256. (b) Gott, A. L.; Piers, W. E.; Dutton, J. L.; McDonald, R.; Parvez, M. *Organometallics* **2011**, *30*, 4236−4249.

(6) (a) Zhang, Y.; Cao, Y.; Leng, X.; Chen, C.; Huang, Z. *Organometallics* **2014**, *33*, 3738−3745. (b) Jian, Z.; Falivene, L.; Wucher, P.; Roesle, P.; Caporaso, L.; Cavallo, L.; Gottker-Schnetmann, I.; Mecking, S. *Chem.—Eur. J.* **2015**, *21*, 2062−2075. (c) Jian, Z.; Mecking, S. *Macromolecules* **2016**, *49*, 4057−4066.

(7) (a) Carrow, B. P.; Nozaki, K. *J. Am. Chem. Soc.* **2012**, *134*, 8802−8805. (b) Carrow, B. P.; Nozaki, K. *Macromolecules* **2014**, *47*, 2541−2555.

(8) Contrella, N. D.; Sampson, J. R.; Jordan, R. F. *Organometallics* **2014**, *33*, 3546−3555.

(9) Sui, X.; Dai, S.; Chen, C. *ACS Catal.* **2015**, *5*, 5932−5937.

(10) Data from ref 9. Conditions: 1 μmol of Pd, 0.5 h, 48 mL of toluene, 2 mL of dichloromethane, 9 atm.

(11) For reviews on allosteric effects in enzyme catalysis: (a) Goodey, N. M.; Benkovic, S. J. *Nat. Chem. Biol.* **2008**, *4*, 474−482. (b) Cornish-Bowden, A. *FEBS J.* **2014**, *281*, 621−632. (c) Tsai, C.-J.; Nussinov, R. *PLoS Comput. Biol.* **2014**, *10*, e1003394. (d) Motlagh, H. N.; Wrabl, J. O.; Li, J.; Hilser, V. J. *Nature* **2014**, *508*, 331−339. For reviews on allosteric effects in synthetic catalysis: (e) Blanco, V.; Leigh, D. A.; Marcos, V. *Chem. Soc. Rev.* **2015**, *44*, 5341−5370. (f) Kovbasyuk, L.; Krämer, R. *Chem. Rev.* **2004**, *104*, 3161−3187. (g) Wiester, M. J.; Ulmann, P. A.; Mirkin, C. A. *Angew. Chem., Int. Ed.* **2011**, *50*, 114−137.

(12) (a) Dydio, P.; Rubay, C.; Gadzikwa, T.; Lutz, M.; Reek, J. N. H. *J. Am. Chem. Soc.* **2011**, *133*, 17176−17179. (b) Mon, I.; Jose, D. A.; Vidal-Ferran, A. *Chem.—Eur. J.* **2013**, *19*, 2720−2725. (c) McGuirk, C. M.; Stern, C. L.; Mirkin, C. A. *J. Am. Chem. Soc.* **2014**, *136*, 4689−4696. (d) Marcos, V.; Stephens, A. J.; Jaramillo-Garcia, J.; Nussbaumer, A. L.; Woltering, S. L.; Valero, A.; Lemonnier, J. F.; Vitorica-Yrezabal, I. J.; Leigh, D. A. *Science* **2016**, *352*, 1555−1559. (e) Kovbasyuk, L.; Pritzkow, H.; Krämer, R.; Fritsky, I. O. *Chem. Commun.* **2004**, 880−881. (f) McGuirk, C. M.; Mendez-Arroyo, J.; d'Aquino, A. I.; Stern, C. L.; Liu, Y.; Mirkin, C. A. *Chem. Sci.* **2016**, *7*, 6674−6683. (g) Tseng, K. T.; Kampf, J. W.; Szymczak, N. K. *ACS Catal.* **2015**, *5*, 411−415. (h) Gianneschi, N. C.; Bertin, P. A.; Nguyen, S. T.; Mirkin, C. A.; Zakharov, L. N.; Rheingold, A. L. *J. Am. Chem. Soc.* **2003**, *125*, 10508−10509. (i) Kita, M. R.; Miller, A. J. M. *J. Am. Chem. Soc.* **2014**, *136*, 14519−14529. (j) McGuirk, C. M.; Mendez-Arroyo, J.; Lifschitz, A. M.; Mirkin, C. A. *J. Am. Chem. Soc.* **2014**, *136*, 16594−16601. (k) Lifschitz, A. M.; Young, R. M.; Mendez-Arroyo, J.; Stern, C. L.; McGuirk, C. M.; Wasielewski, M. R.; Mirkin, C. A. *Nat. Commun.* **2015**, *6*, 6541. (l) Smith, A. J.; Kalkman, E. D.; Gilbert, Z. W.; Tonks, I. A. *Organometallics* **2016**, *35*, 2429−2432. (m) Chen, M.; Zou, W.; Cai, Z.; Chen, C. *Polym. Chem.* **2015**, *6*, 2669−2676.

(13) (a) Komon, Z. J. A.; Bu, X.; Bazan, G. C. *J. Am. Chem. Soc.* **2000**, *122*, 1830−1831. (b) Komon, Z. J. A.; Bu, X.; Bazan, G. C. *J. Am. Chem. Soc.* **2000**, *122*, 12379−12380. (c) Lee, B. Y.; Bazan, G. C.; Vela, J.; Komon, Z. J. A.; Bu, X. *J. Am. Chem. Soc.* **2001**, *123*, 5352−5353. For related work, see: (d) Lee, B. Y.; Bu, X.; Bazan, G. C. *Organometallics* **2001**, *20*, 5425−5431. (e) Boardman, B. M.; Bazan, G. C. *Acc. Chem. Res.* **2009**, *42*, 1597−1606. (f) Lee, B. Y.; Kim, Y. H.; Shin, H. J.; Lee, C. H. *Organometallics* **2002**, *21*, 3481−3484. (g) Shim, C. B.; Kim, Y. H.; Lee, B. Y.; Dong, Y.; Yun, H. *Organometallics* **2003**, *22*, 4272−4280. (h) Shim, C. B.; Kim, Y. H.; Lee, B. H.; Shin, D. M.; Chung, Y. K. *J. Organomet. Chem.* **2003**, *675*, 72−76. (i) Kim, Y. H.; Kim, T. H.; Lee, B. Y.; Woodmansee, D.; Bu, X.; Bazan, G. C. *Organometallics* **2002**, *21*, 3082−3084. (j) Boardman, B. M.; Valderrama, J. M.; Munoz, F.; Wu, G.; Bazan, G. C.; Rojas, R. *Organometallics* **2008**, *27*, 1671−1674. (k) Chen, Y.; Boardman, B. M.; Wu, G.; Bazan, G. C. *J. Organomet. Chem.* **2007**, *692*, 4745−4749. (l) Azoulay, J. D.; Rojas, R. S.; Serrano, A. V.; Ohtaki, H.; Galland, G. B.; Wu, G.; Bazan, G. C. *Angew. Chem., Int. Ed.* **2009**, *48*, 1089−1092. (m) Azoulay, J. D.; Koretz, Z. A.; Wu, G.; Bazan, G. C. *Angew. Chem., Int. Ed.* **2010**, *49*, 7890−7894. (n) Kwon, H. Y.; Lee, S. Y.; Lee, B. Y.; Shin, D. M.; Chung, Y. K. *Dalton Trans.* **2004**, 921−928. (o) Chen, Y.; Wu, G.; Bazan, G. C. *Angew. Chem., Int. Ed.* **2005**, *44*, 1108−1112. (p) Boardman, B. M.; Wu, G.; Rojas, R.; Bazan, G. C. *J. Organomet. Chem.* **2009**, *694*, 1380−1384. (q) Kim, Y. H.; Kim, T. H.; Kim, N. Y.; Cho, E. S.; Lee, B. Y.; Shin, D. M.; Chung, Y. K. *Organometallics* **2003**, *22*, 1503−1511. (r) Okada, M.; Nakayama, Y.; Shiono, T. *J. Organomet. Chem.* **2007**, *692*, 5183−5189. (s) Okada, M.; Nakayama, Y.; Ikeda, T.; Shiono, T. *Macromol. Rapid Commun.* **2006**, *27*, 1418−1423. (t) Okada, M.; Nakayama, Y.; Shiono, T. *Macromol. Chem. Phys.* **2014**, *215*, 1792−1796.

DOI: 10.1021/acs.organomet.7b00815
Organometallics 2017, 36, 4990−5002

(14) Cai, Z.; Shen, Z.; Zhou, X.; Jordan, R. F. *ACS Catal.* **2012**, *2*, 1187−1195.
(15) Reisinger, C. M.; Nowack, R. J.; Volkmer, D.; Rieger, B. *Dalton Trans.* **2007**, 272−279.
(16) Nowack, R. J. Neutral Nickel and Palladium Complexes as Catalysts in Copolymerizations of Polar and Non-Polar Monomers. Dissertation, Universitat Ulm, Ulm, Germany, 2008.
(17) Fenske, D.; Mattes, R.; Löns, J.; Tebbe, K.-F. *Chem. Ber.* **1973**, *106*, 1139−1144.
(18) Grice, I. D.; Jenkins, I. D.; Busfield, W. K.; Byriel, K. A.; Kennard, C. H. L. *Acta Crystallogr., Sect. E: Struct. Rep. Online* **2004**, *60*, o2384−o2385.
(19) Vela, J.; Lief, G. R.; Shen, Z.; Jordan, R. F. *Organometallics* **2007**, *26*, 6624−6635.
(20) The C39−C44 C_6F_5 ring and the C27−C32 Ph ring are organized in an eclipsed parallel arrangement with a distance of 3.66 Å between the ring centroids. The C27−C32 and C15−C20 Ph rings adopt a parallel-displaced orientation (angle between planes 10.9°) with an interplane distance of ca. 3.3 Å and an intercentroid distance of 4.02 Å.
(21) (a) Hunter, C. A.; Sanders, J. K. M. *J. Am. Chem. Soc.* **1990**, *112*, 5525−5534. (b) Wheeler, S. E. *Acc. Chem. Res.* **2013**, *46*, 1029−1041. (c) Tsuzuki, S.; Uchimaru, T.; Mikami, M. *J. Phys. Chem. A* **2006**, *110*, 2027−2033. (d) Wang, W.; Zhang, Y.; Wang, Y.-B. *Int. J. .Quantum Chem.* **2017**, *117*, e25345−e25351. (e) Sherrill, C. D. *Acc. Chem. Res.* **2013**, *46*, 1020−1028.
(22) Ellis, D. D.; Harrison, G.; Orpen, A. G.; Phetmung, H.; Pringle, P. G.; deVries, J. G.; Oevering, H. *J. Chem. Soc., Dalton Trans.* **2000**, 671−675.
(23) Zhuang, R.; Xu, J.; Cai, Z.; Tang, G.; Fang, M.; Zhao, Y. *Org. Lett.* **2011**, *13*, 2110−2113.
(24) Krawczyk, H. *Synth. Commun.* **1997**, *27* (18), 3151−3161.
(25) Exchange of the Pd-bound (O1, Figures 1, 4, and 5) and non-Pd-bound oxygen (O2) atoms is fast on the NMR time scale for **2a-lut**, **2b-lut/py**, **2c-lut/py**, and **2d-py** at room temperature, resulting in the presence of a single set of ^{1}H resonances for the PAr_2 groups, as well as for the diastereotopic −OCH_2CH$_3$ hydrogens in **2b-lut/py** and the diastereotopic −OCHMe_2 groups in **2c-lut/py** and **2d-py**. The barrier to this exchange process for **2b-py** was determined to be $\Delta G^{\ddagger}$ = 10.5 kcal mol^{-1} from the coalescence of the −OCH_2CH$_3$ resonances (500 MHz, δ 3.47, 2.49, T_c = 238 K). *Cis/trans* isomerization of (PO)PdR(CH$_2$═CH$_2$) species is believed to precede the migratory insertion step in chain growth by (PO)PdR catalysts. One proposed isomerization mechanism, which was predicted to have a low barrier, involves coordination of a second sulfonate oxygen atom to Pd to generate a (κ^3-*P*,*O*,*O*-PO)PdR(CH$_2$═CH$_2$) species, followed by Berry pseudorotations and formation of the isomerized (κ^2-*P*,*O*-PO)PdR(CH$_2$═CH$_2$) product. While the exchange of Pd-bound and non-Pd-bound sulfonate oxygen atoms has not been experimentally observed in (PO)PdMeL systems, the present results suggest that this process is indeed facile. See refs 1, 3, and (a) Zhou, X.; Lau, K.; Petro, B. J.; Jordan, R. F. *Organometallics* **2014**, *33*, 7209−7214. (b) Conley, M. P.; Jordan, R. F. *Angew. Chem., Int. Ed.* **2011**, *50*, 3744−3746.
(26) Flack, H. D. *Helv. Chim. Acta* **2003**, *86*, 905−921.
(27) The C23−C28 C_6F_5 ring and the C8−C13 Ph ring are organized in an eclipsed parallel arrangement with a distance of 3.58 Å between the ring centroids.
(28) Shen, Z.; Jordan, R. F. *J. Am. Chem. Soc.* **2010**, *132*, 52−53.
(29) In a control ethylene polymerization, the catalyst **2b-py** + 2B(C_6F_5)$_3$·Et$_2$O exhibited similar activity and produced PE with similar MW as **5b**/**5b′**, showing that the Et$_2$O has only a minimal effect on catalyst performance (see the Supporting Information for details).
(30) (a) Nakano, R.; Chung, L. W.; Watanabe, Y.; Okuno, Y.; Okumura, Y.; Ito, S.; Morokuma, K.; Nozaki, K. *ACS Catal.* **2016**, *6*, 6101−6113 (b).
(31) The Pd1−O1 distances of **3a-lut** and **3b-lut** are very similar to that in **A** (2.164(7) Å; R = Ph; L = py), which suggests that the donor ability of the borane-coordinated phosphinate/phosphonate group is similar to that of the sulfonate group. Piche, L.; Daigle, J.-C.; Poli, R.; Claverie, J. P. *Eur. J. Inorg. Chem.* **2010**, *2010*, 4595−4601.
(32) Liu, W.; Malinoski, J. M.; Brookhart, M. *Organometallics* **2002**, *21*, 2836−2838. (b) Malinoski, J. M.; Brookhart, M. *Organometallics* **2003**, *22*, 5324−5335. (c) DiRenzo, G. M.; White, P. S.; Brookhart, M. *J. Am. Chem. Soc.* **1996**, *118*, 6225−6234.
(33) Falivene, L.; Credendino, R.; Poater, A.; Petta, A.; Serra, L.; Oliva, R.; Scarano, V.; Cavallo, L. *Organometallics* **2016**, *35*, 2286−2293.
(34) The C1−Pd1−N1 angles can be used to assess lateral steric pressure but appear to be influenced by packing forces in these complexes. The presence of a CH_2Cl_2 solvent molecule in the mouth of the C1−Pd1−N1 angle in **2a-lut**, an intermolecular π-stacking interaction between 2,6-lutidine ligands (3.78 Å intercentroid distance) in **2b-lut**, and an intermolecular π-stacking interaction between a C_6F_5 ring and the 2,6-lutidine ring (4.0 Å intercentroid distance) in **3a-lut** likely influence the C1−Pd1−N1 angles in these complexes and complicate comparison of these parameters.
(35) The Lewis acidities of B(C_6F_5)$_3$ and BF_3 are similar. (a) Massey, A. G.; Park, A. J. *J. Organomet. Chem.* **1966**, *5*, 218−225. (b) Beckett, M. A.; Brassington, D. S.; Coles, S. J.; Hursthouse, M. B. *Inorg. Chem. Commun.* **2000**, *3*, 530−533. (c) Komon, Z. J. A.; Bazan, G. C.; Fang, C.; Bu, X. *Inorg. Chim. Acta* **2003**, *345*, 95−102. (d) Sivaev, I. B.; Bregadze, V. I. *Coord. Chem. Rev.* **2014**, *270*−*271*, 75−88. (e) Mendez, M.; Cedillo, A. *Comput. Theor. Chem.* **2013**, *1011*, 44−56. (f) Jacobsen, H.; Berke, H.; Doring, S.; Kehr, G.; Erker, G.; Frohlich, R.; Meyer, O. *Organometallics* **1999**, *18*, 1724−1735.
(36) Assuming that, for **2d-py**, R_{growth} and $R_{transfer}$ are both increased by a factor of 6 by generation of the base-free species (cf. results for **2a-lut** and **2b-lut**), R_{growth} and $R_{transfer}$ are increased by a ca. factor of 100 and 10, respectively, by coordination of B(C_6F_5)$_3$ to the PPO$^-$ ligand, which at 80 °C corresponds to $\Delta\Delta G^{\ddagger}$ of 1.1 kcal mol^{-1}.
(37) De Graaf, W.; Boersma, J.; Smeets, W. J. J.; Spek, A. L.; Van Koten, G. *Organometallics* **1989**, *8*, 2907−2917.

DOI: 10.1021/acs.organomet.7b00815
Organometallics 2017, 36, 4990−5002